Coastal Vulnerability along the Northumberland Strait, the Municipality of the County of Cumberland and Statistical Methods and Data Sources to Calculate Return Periods of Water Levels

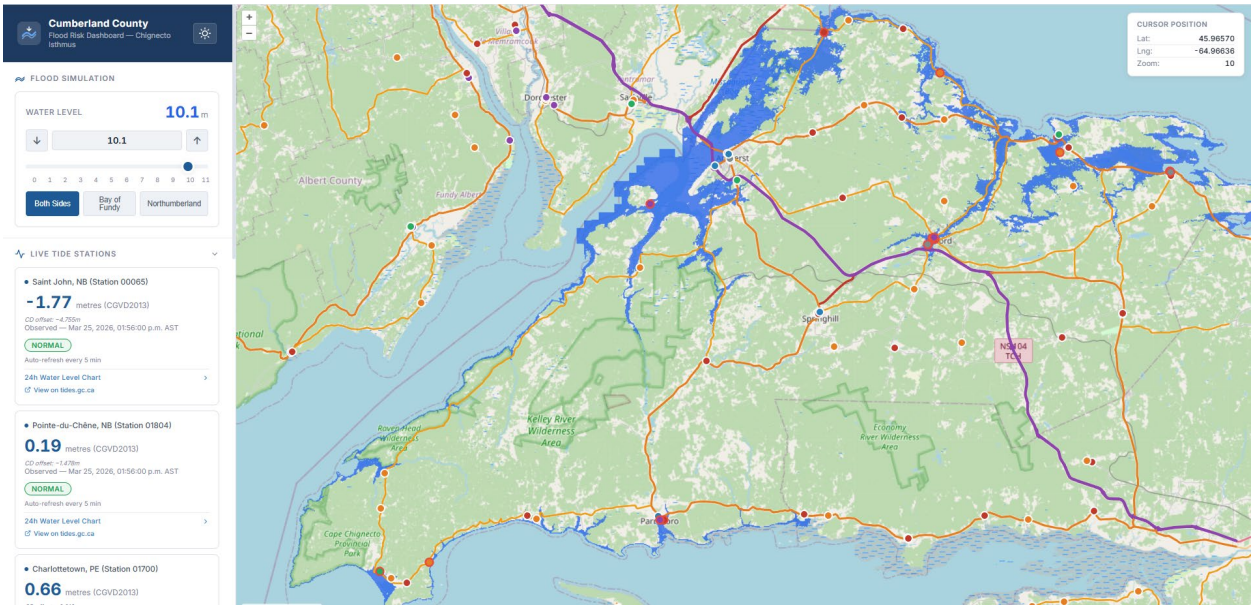

Tim Webster, Thomas Allen, Cale Stevens, Sean Dzafovic, and the Geospatial Data Analytics students
Nova Scotia Community College
Applied Geomatics Research Group
NSCC, Middleton, NS
Tel. 902 825 5475
Email: timothy.webster@nscc.ca

Maggie Pitts GIS Analyst, Municipality of the County of Cumberland, 1395 Blair Lake Rd, Amherst, NS B4H 3Y4

How to cite this work and report:

NSCC Applied Geomatics Research Group. 2026. Coastal Vulnerability along the Northumberland Strait, the Municipality of the County of Cumberland and Statistical Methods and Data Sources to Calculate Return Periods of Water Levels, Applied Geomatics Research Group, NSCC Middleton, NS.

Copyright and Acknowledgement

The Applied Geomatics Research Group of the Nova Scotia Community College maintains full ownership of all data collected by equipment owned by NSCC and agrees to provide the end user who commissions the data collection a license to use the data for the purpose they were collected for upon written consent by AGRG-NSCC. The end user may make unlimited copies of the data for internal use; derive products from the data, release graphics and hardcopy with the copyright acknowledgement of **"Data acquired and processed by the Applied Geomatics Research Group, NSCC"**. Data acquired using this technology and the intellectual property (IP) associated with processing these data are owned by AGRG/NSCC and data will not be shared without permission of AGRG/NSCC.

Table of Contents

Table of Figures

List of Tables

1 Introduction

This project was funded by Research Nova Scotia, under their Atlantic Climate Research Collaboration (ACRC) fund which was awarded in the summer of 2023. This project utilized lidar data to construct a high-resolution elevation model for the Municipality of the County of Cumberland's (MCC) coastal area. Provincial guidelines were used for generating coastal flood hazard maps. The guidelines are based on Higher High Water Large Tide (HHWLT) plus the 1:20-year and 1:100-year storm surge return periods for present day. As well, flooding into the future will be considered by examining relative sea-level rise (RSL) and the possible collapse of the Antarctic ice sheet for the years 2050, 2100 and 2150. We also supplied and installed a tide gauge at one of the wharfs in the MCC. The MCC is bounded by the ocean on two sides, to the north the Northumberland Strait, which is vulnerable to some of the largest storm surges that occur in the region, and to the south by the Bay of Fundy, which hosts the highest tides in the world and is adjacent to the main trade corridor that Nova Scotia depends on to ship and receive goods. We have examined the tide gauge records in the region and calculated the return periods of total water level as well as residual (storm surge) levels from the gauges. Also, we have reviewed other sources of return period information based on hindcast modelling. The project deliverables and report were delivered to the MCC and funder. As well, a web-based dashboard was constructed and hosted at NSCC-AGRG for the project to facilitate access to these data. In addition to the deliverables specific to this project, NSCC-AGRG included other climate change related coastal studies they have done in the MCC during the past decade. The project also funded a MSc student, Fatma Sarhan under the supervision of Dr. Orla Murphy in the Math and Statistics Department at Dalhousie University. Her thesis involves examining tide gauge records and return periods and the ability to estimate return periods for areas that lie between tide gauges like the MCC.

The MCC will use these data in three important ways. First, up to date estimates of return periods for various high-water levels will inform revisions of the Emergency Management Plan and will help the MCC to effectively allocate and fund response resources, such as personnel, equipment, and shelters. Perhaps more importantly, it will greatly enhance the MCC's efforts aimed at improving public awareness and individual and family preparedness. Second, the data will be used to generate maps that will enable the MCC to improve and adjust its land use regulations, so that new development does not unknowingly put lives and investments at risk. The MCC has set-back requirements now, but the lack of detailed data has dictated a broad-brush approach. The regulations will be improved and fine-tuned with high-resolution flood hazard data. Developers claim the current regulations unnecessarily restrict development, and without good data to scientifically justify where the restrictions are imposed, they are very difficult to defend, especially at the political level. Third, these data will also be used for asset management. It will guide where new or upgraded infrastructure such as water treatment plants, roads, health care facilities, schools, etc., are placed. For example, the MCC has several wastewater treatment facilities very close to the shore. One, in the community of Wallace, is

located on former salt marsh protected by a dyke and is due for a capital-intensive lagoon refurbishment in the next few years. The data from this study will help the MCC decide if the plant and lagoon should be relocated or protected in some other way.

The project consisted of several components that will be described in the following sections. The provincial lidar DEM was utilized to build static bathtub flood hazard layers for both the Northumberland and Bay of Fundy coasts of the MCC. The lidar DEM for the MCC was used to construct a colour shaded relief (CSR) map for the MCC which can be used as a backdrop to better understand the terrain. A tide gauge was delivered and installed at Northport in collaboration with the MCC to measure coastal water levels. An analysis of storm surge and total water level return periods was examined. This component of the project was executed by both researchers at AGRG-NSCC and from Dalhousie through funding an MSc student mentioned earlier. The MSc thesis will be delivered in the summer of 2026. Researchers at AGRG have built a set of tools to analyse the tide gauge data from the various locations in the Martimes and compute the return periods of both total water level (tide + surge) and storm surge alone. These data will be presented in the following sections. One of the biggest challenges for many Nova Scotian communities is to determine these values if they are not close to one of the existing tide gauges. For this we have also examined return periods that have been derived from hindcast models of storm surge and compared the results to actual empirical gauge data. Lastly, although not explicitly defined in the project proposal, we have constructed a dashboard to allow access to various data for the MCC including the data generated for this project as well as past projects AGRG has been involved with. This dashboard was constructed by students from the Geospatial Data Analytics program as part of their course work. The students involved were Rose Boudreau, Cohen Hanley, Maggie Lingley and Justin Monteith and organized by NSCC Applied Research Student Innovation Coordinator, Beth Easson.

2 Methods

2.1 Static Coastal Flood Layer Construction

A 1 m lidar-based Digital Elevation Model (DEM) from GeoNOVA served as the basis for the flood layers created for the MCC. The DEM can be shaded to provide a more enhanced look at the terrain (Figure 1). This raster provided a detailed representation of the three-dimensional surface of the study area. While flood levels can be represented by a “bathtub model” by determining the area covered by a hypothetical surface at a fixed elevation, this can produce inaccurate results. Bridges and elevated roadbeds, for example, will serve to block the flow of water in the raster model and will show water collecting in incorrect areas where water would flow unimpeded under a bridge or through a culvert. To more closely model flood conditions, these features will need to be accounted for by “hydro-conditioning” the raster. This process

involves examining the raster in conjunction with a basemap or imagery to determine the path of small rivers or streams. A map feature is created to indicate a candidate path for water to flow. Care must be taken during this process that the feature is wide enough for water to move through regardless of orientation. A narrow connection feature on a 45-degree angle will probably result in a series of 1m pixels that are not orthogonally connected, which will prevent water flowing in the model and result in an incorrect flood level representation.

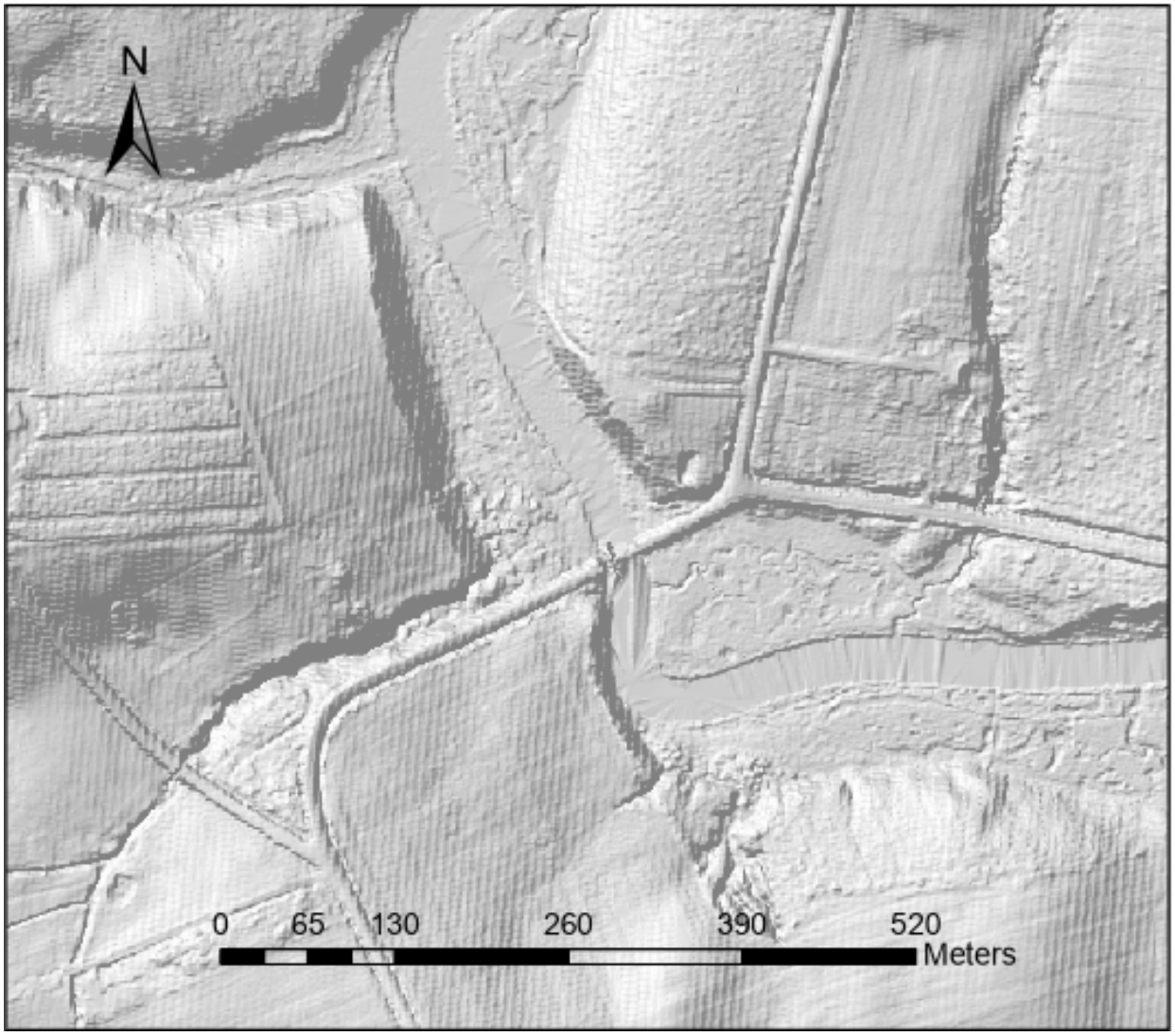

Figure 1 Example of a shaded relief map of the lidar DEM. Note there appears to be artifacts withing the data visible in cleared areas.

After all the crossing points are determined, the raster will be altered by creating an artificially low elevation where the connecting lines are located. For this model, the elevation value at the connecting points was set to -5 m (Figure 2). The low points will automatically fill when the water level reaches the connection, but the flood level will not spread until the water level exceeds the elevation of the surrounding terrain. The same process can be used to simulate

coastal flooding by artificially removing flood management structures such as aboiteaux or breaching berms.

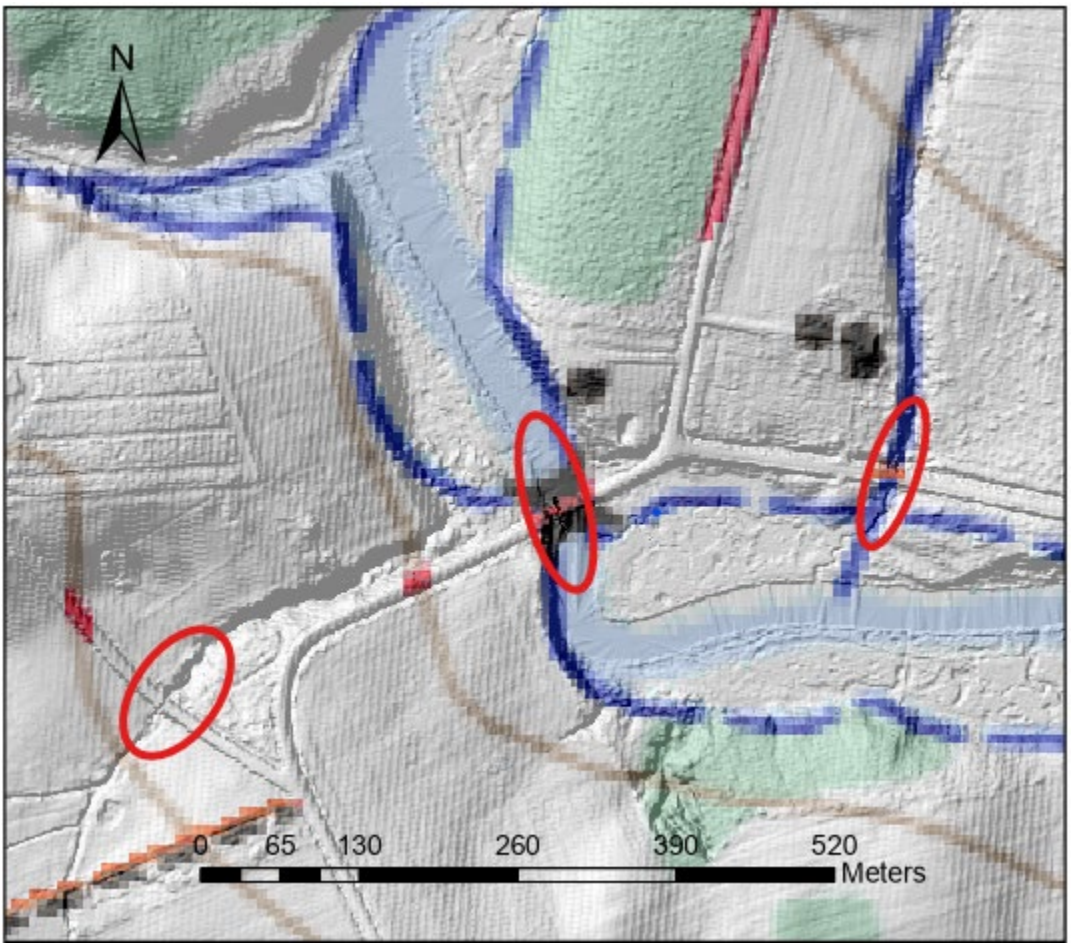

Figure 2 Lidar DEM shaded relief with NTS 50k map underneath. Hydro-connection shapefile points circled in red.

The ocean areas to the north had a changing, non-zero elevation. This indicates the lidar data used to create the raster was not collected at low tide, and the lidar captured waves and changing tide levels which were incorporated into the original GeoNOVA raster. As this would impede the proper functioning of the flood modelling script, this raster was further altered by forcing the ocean areas to the north of the study area to have an elevation of 0m.

After the alterations to the raster were completed, an arbitrary source point was marked with a point shapefile in an ocean area of the raster. The only factor in the position of this point is that it needs to have unimpeded access to all areas of the coast.

As the MCC takes up the entire Chignecto Isthmus, NSCC-AGRG's proprietary flood tool was run twice, with separate flood sources in the Bay of Fundy and the Northumberland Strait. In both cases, the parameters for the flood layers were from 0 – 15 m, with an interval of 0.1 m. Two examples of the derived flood hazard layers are shown in Figure 3 and Figure 4.

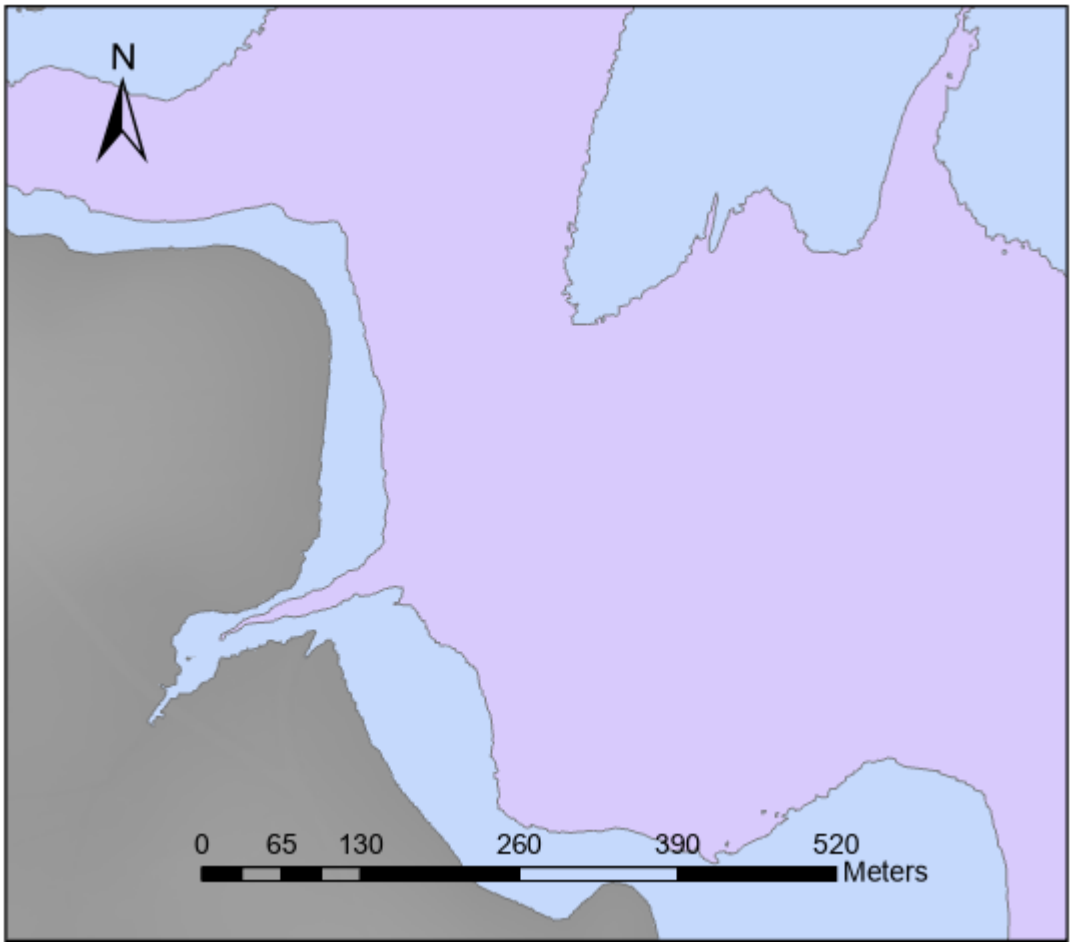

Figure 3 Example of flood inundation layers, 9.7 m (purple) and 14.0 m (blue) flood layers

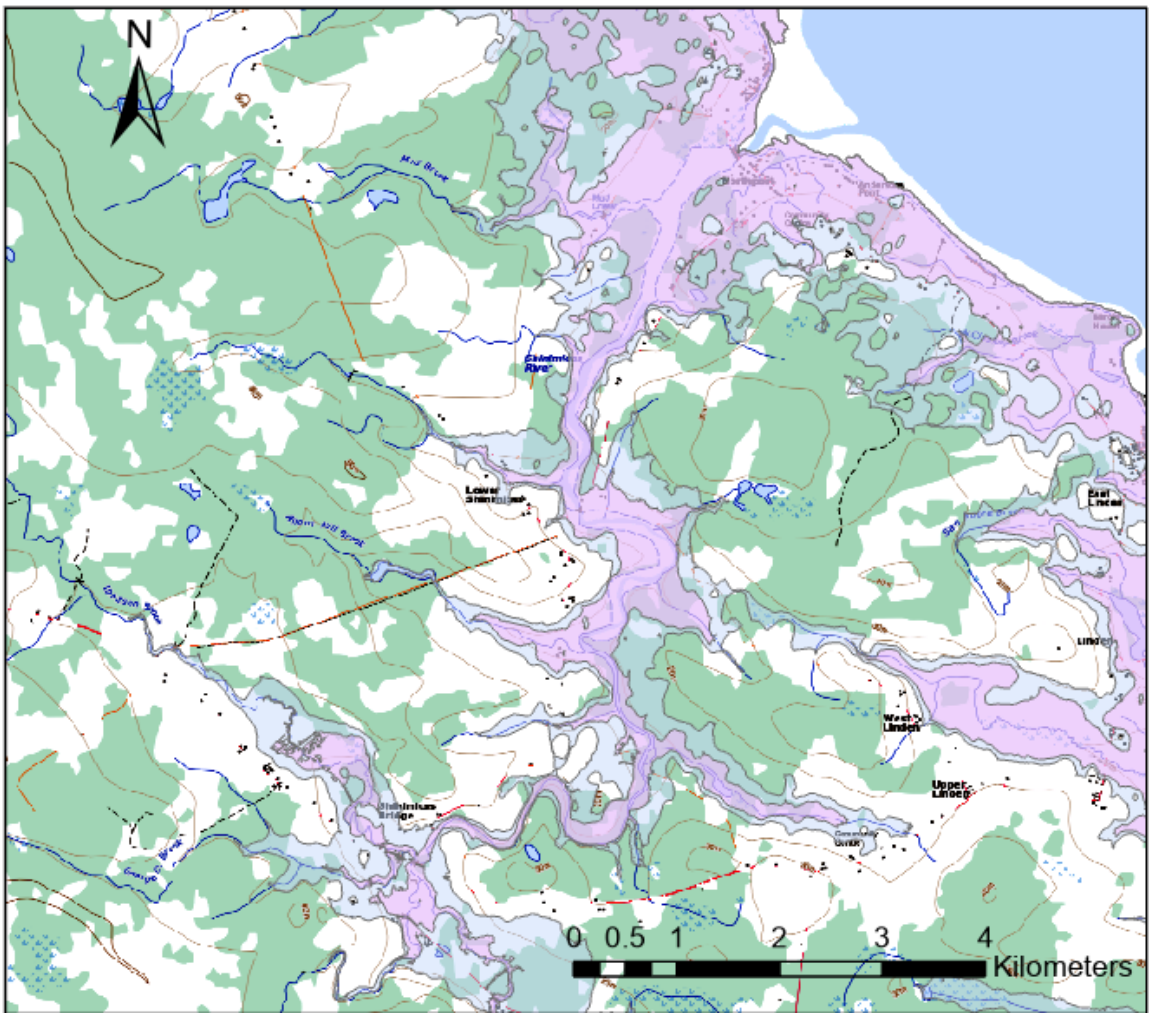

Figure 4 More examples of flood hazard layers, 14.0m (blue) and 9.7m (purple) flood layers superimposed on NTS 50k map. Northport at top of map.

The Nova Scotia Coastal Flood Hazard standard involves starting with the Higher high Water large Tide (HHWLT) elevation relative to CGVD2013, then adding the water level of the 1 in 20 and 1 in 100-year storm surges. To consider future flood hazard levels the current values are used and the relative sea level rise is added to them. In 2100 there is also a risk that the western Antarctica ice sheet may collapse, thus an additional 65 cm is added (Table 1).

Table 1 Coastal flood hazard layers, Northumberland and Fundy shore, present day and 2050, 2100 considering climate change, relative sea level rise and possible collapse of the Antarctica Ice Sheet (AA).

		Northumberland CGVD2013		Fundy CGVD2013	
	Projection	Value	Flood Layer	Value	Flood Layer
Present	20 Year	2.66 m	2.7 m	15.55 m	15.6 m
	100 Year	2.96 m	3.0 m	18.23 m	18.2 m
2050	20 Year	3.1 m	3.1 m	15.98 m	16.0 m
	100 Year	3.4 m	3.4 m	19.09 m	19.1 m
2100	20 Year	3.9 m	3.9 m	16.78 m	16.8 m
	100 Year	4.2 m	4.2 m	20.29 m	20.3 m
2100 AA	20 Year	4.55 m	4.6 m	17.43 m	17.4 m
	100 Year	4.85 m	4.9 m	21.99 m	22.0 m

2.2 Colour Shaded Relief (CSR) Map of Municipality of the County of Cumberland

NSCC-AGRG utilized the 1m DEM to build the colour shaded relief map of the MCC. An area comprising the MCC and some adjacent ocean areas was copied from the source raster. This clip had elevations ranging from -51 m to 333 m. The floating-point elevation values were scaled from -8 to 365 m to 0 to 255 and pseudo-colour was applied where the break between blue and green occurs at the 0 m elevation CGVD2013. The colour ramp is designed to aid the eye in interpreting elevation from green (low) through yellow and red-magenta for the highest terrain. The terrain was then shaded from the northwest (azimuth 315 degrees) and a 45-degree angle with a 5-times vertical exaggeration applied. The pseudo-coloured elevation was written to three bands representing the colour in RGB and merged with the shaded relief to build a colour shaded relief model to be used for visual interpretation (Figure 5).

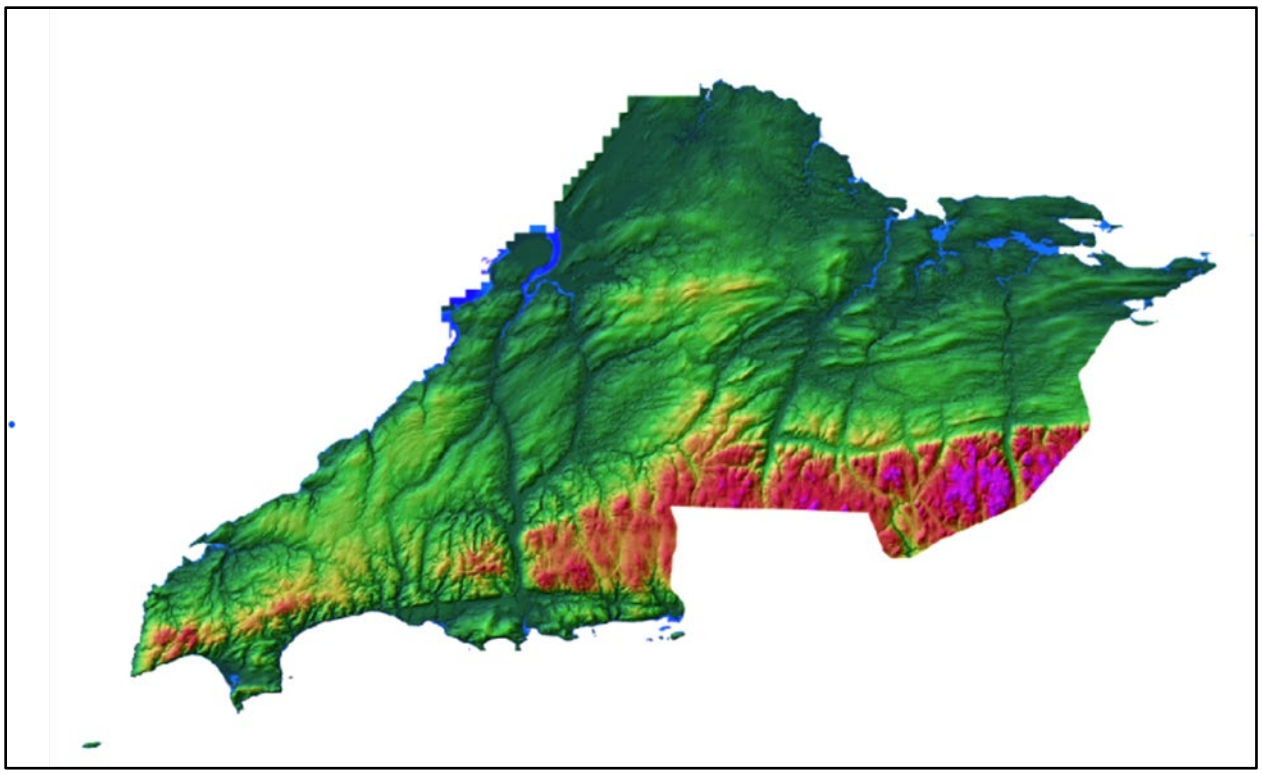

Figure 5 Colour Shaded Relief Map of the County of Cumberland

2.3 Return Period Calculations

Return periods were estimated for the flood planes using extreme value analysis using data from tide gauges. After cleaning, the data were sampled annually and fitted to block-maxima distributions. Return periods were then calculated as the exceedance probability of the cumulative distribution functions of the distributions.

Tide Gauge Data

Tide observation data were retrieved from https://tides.gc.ca. Historical predictions (recorded before current API) had to be requested. These predictions were generated using harmonic analysis of tidal signals. The nearest tide stations to the MCC with sufficient record length were Shediac Bay and Saint John. As such, the calculated return periods must be interpolated to estimate the return period on the coast of the MCC.

Cleaning Data

Some tide gauges contained significant errors. There were many phase offsets, single-hour errors, and other artifacts. Without cleaning, these errors heavily affected the return period results. Shediac Bay was acceptable, however Saint John had significant errors.

Total water level return periods were largely unaffected, due to sampling annual maxima. Phase offsets do not affect these, and single-record errors (Figure 6) are easy to detect (or are not significant enough to affect the analysis). The only errors that can affect annual maxima are

those that push the annual maxima higher than the real value, which were usually caused by an easily identifiable single-record spike.

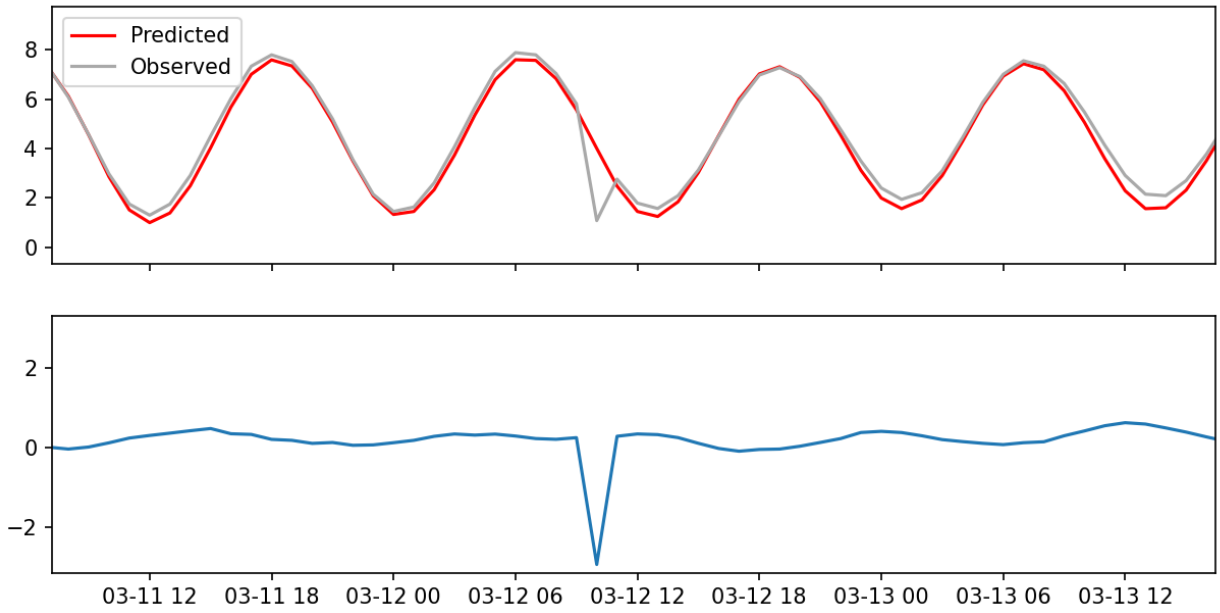

Figure 6 – A single-record error in the Saint John tide gauge in 1951. The top graph is observed (gray) vs predicted (red) water levels in Chart Datum. The bottom graph is the residual difference between the observed and the predicted.

Residuals are heavily affected by tide gauge errors. Any kind of error in the tide gauge that causes it to deviate from the predicted tide will cause residuals to increase significantly (Figure 7). Some errors are easily identifiable (e.g., phase offsets, single-record spikes), however it becomes increasingly difficult to determine which records are errors and which are from a real event. Even after significant cleaning, the residual return periods produced from analyzing the gauge data are questionable.

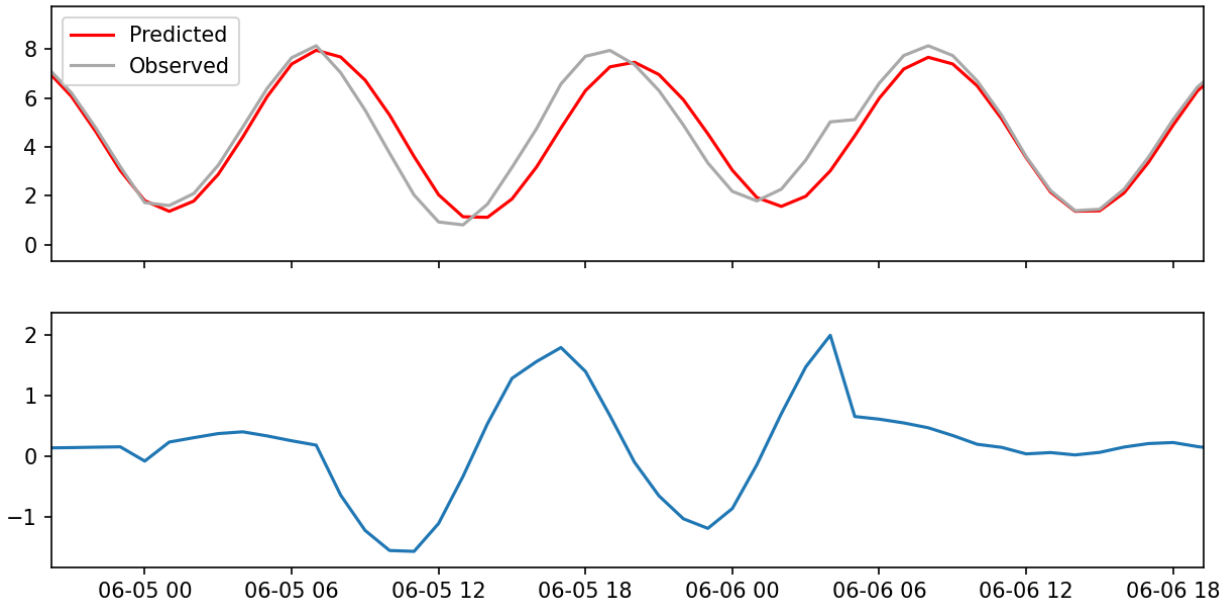

Figure 7 – A phase offset found in the Saint John tide gauge in 1950. The top graph is observed (gray) vs predicted (red) water levels in Chart Datum. The bottom graph is the residual difference between the observed and the predicted. Note how the phase offsets causes the residuals to increase despite no real surge occurring. The start and end of this offset are apparent (see sharp spike on 06-05 06 and flat section at 06-06 03), however this is not always the case.

In addition to the aforementioned errors, the Saint John tide gauge contained unique errors that required removal. One such error was a bottoming out of the tide gauge from 1997 to 2000 (Figure 8). A much stranger error was in a section of the 2014 data where the amplitude of the observed water level shrank, causing low tide to appear higher and high tide to appear lower (Figure 9). Both errors were cut from the record.

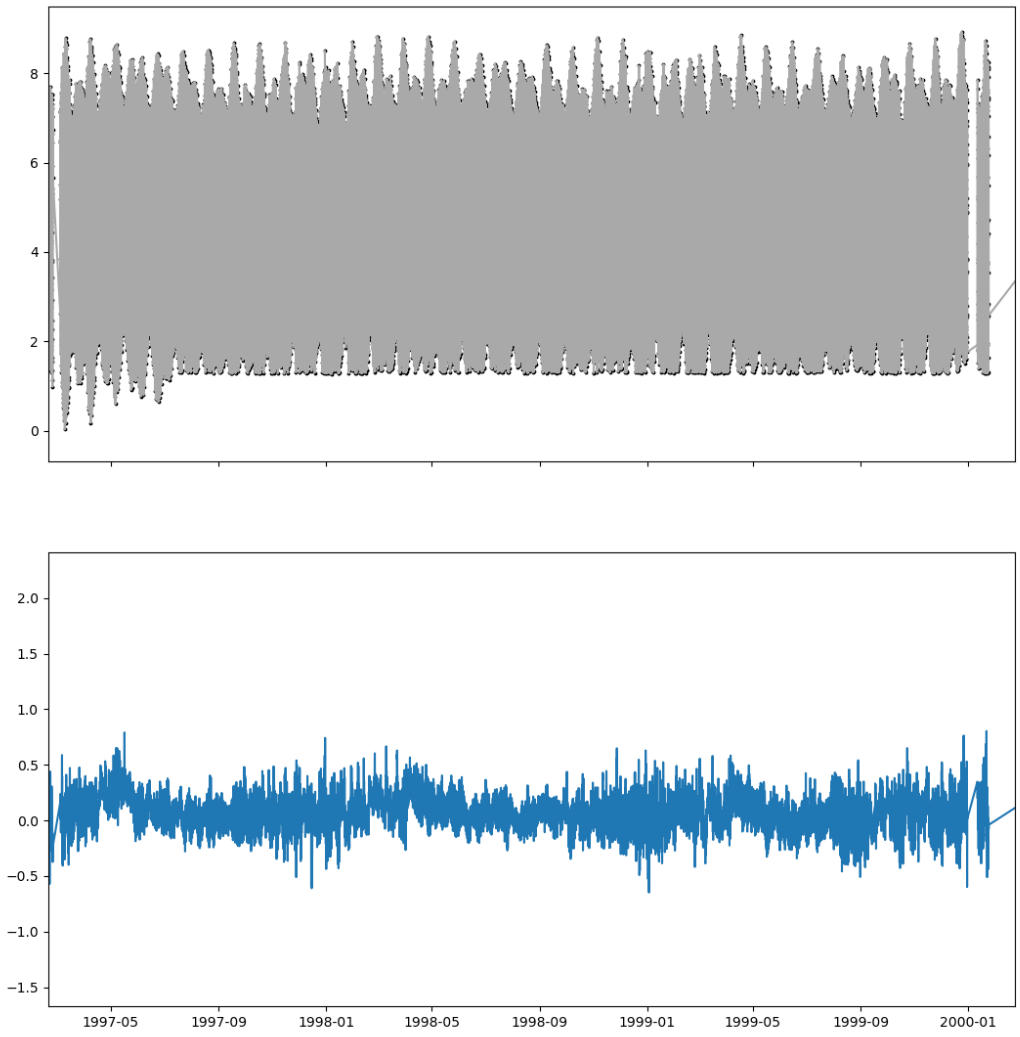

Figure 8 – The Saint John tide gauge bottoming out from 1997 to 2000. The top graph is observed water level in Chart Datum. The bottom graph is the residual difference between the observed and the predicted. The error is not apparent in the residuals, indicating the predictions were influenced by the gauge bottoming out.

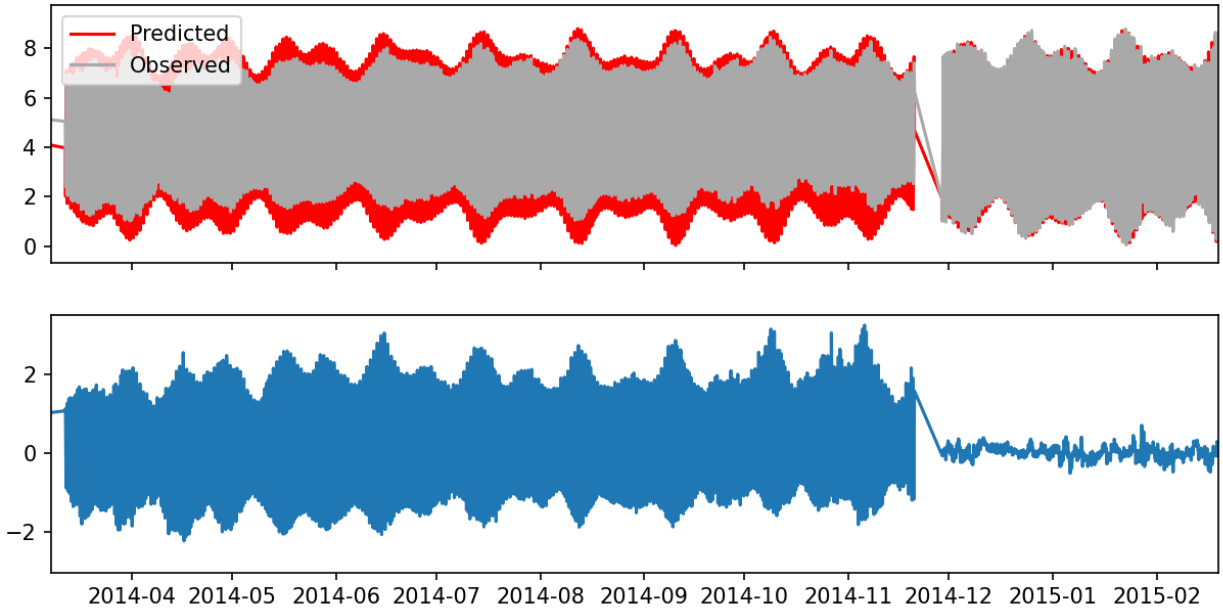

Figure 9 – The Saint John tide gauge in 2014. The top graph is observed (gray) vs predicted (red) water levels in Chart Datum. The bottom graph is the residual difference between the observed and the predicted. It is visually apparent that the observed water levels in 2014 had a lower amplitude than they should have.

Fixing Errors

The errors found in the gauge data were either corrected or removed from the gauge. While some errors were obvious due to their size (Figure 8), others required algorithmic assistance to be detected.

The Normalized Difference Ratio $\frac{a-b}{a+b}$ is a useful metric for identifying sharp changes in slope. By calculating the slope at each record and comparing it to neighboring records, sharp spikes are highlighted. This ratio was applied on the residuals, which better highlight issues in the record. The flagged records were usually single-record spikes, however care must be exercised to identify false-positives such as sudden storm surges. Spikes can be further identified by looking for adjacent high slopes. A single spike would be expected to produce a sudden slope change in one direction, immediately followed by a sudden slope change in the other direction. This removes some false positives.

Detrend

Tidal predictions do not account for sea level rise and project into the past assuming the sea level was the same as it was when the predictions were generated (i.e., the epoch). The observation data include an upwards trend due to sea level rise and crustal subsidence and therefore must be normalized to the epoch of the predictions using a linear detrend (Figure 10).

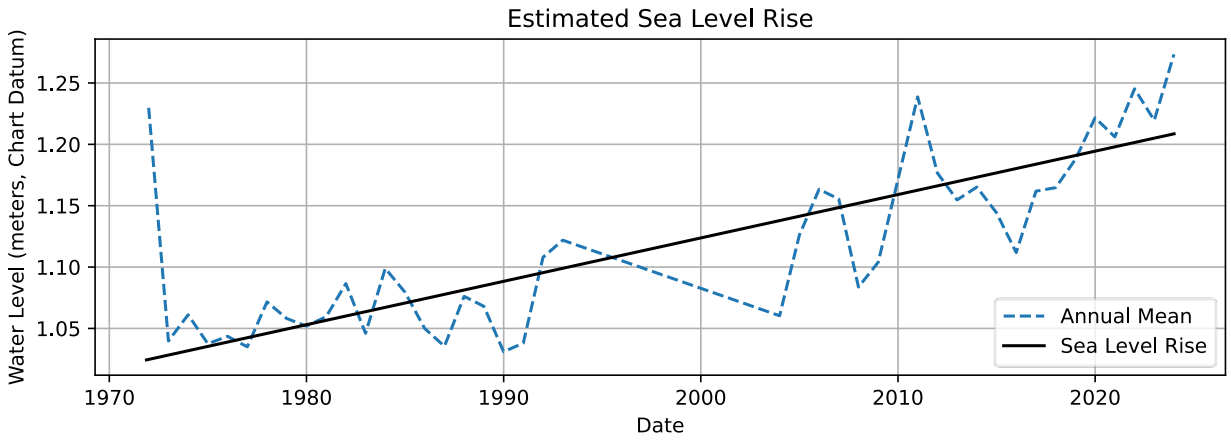

Figure 10 – The estimated sea level rise of Saint John based on annual mean sea level. The y offset of the black line was selected for illustrative purposes only, as it is only meant to convey slope.

Model Generation

Many common statistical distributions (e.g., Gumbel, Weibull, GEV, etc.) are classified as "block-maxima" distributions, meaning all the records you use to fit the distributions are assumed to have a unit length of 1. For example, when fitting a Gumbel distribution with a list of maxima, the distribution inherently assumes each record was selected from non-overlapping date ranges of the same size (e.g., one year). This approach is simple to implement, however it has the disadvantage of missing multiple extreme events in the same date range.

Model Analysis

Root mean square (RMS) and correlation statistics are generated for all fitted distributions by comparing the cumulative distribution functions (CDF) from the empirical data and fitted distributions. A lower RMS indicates that a model fits the observations well, and a higher correlation indicates the shape of the distribution matches the shape of the observations well.

The CDF is a function that defines the probability of a random sample being lower or equal to a given value. CDF probabilities are represented as decimal values between 0 and 1, with 1 being 100% probability and 0 being 0%. Each statistical distribution has its own equation CDF equation that is used to determine probabilities.

An empirical CDF is generated using the Weibull plotting positions $\boldsymbol{F_i = \frac{i}{n+1}}$, where $\boldsymbol{n}$ is the number of annual maxima. This allows direct comparing of the fitted distributions to the observed records.

The return period for a block-maxima distribution is defined as the inverse of the exceedance probability per block, in the unit of the block-size (e.g., 1 year). For instance, if the probability of exceeding 4.2 meters is 0.5 and the block-size of the model is one year, then the return period would be 1 / 0.5, which evaluates to 2 years.

The empirical CDF can be used to generate an empirical return period by calculating the inverse of the exceedance probability (1 / 1 - CDF). These return periods can then be plotted directly on top of the return period plots to show the return periods of real-world events.

Shediac Bay

Total water level return periods for Shediac Bay closely matched the empirically calculated return values (Figure 11). The Gumbel model offered the preferred return periods due to having the least overestimation. The modelled return periods are presented in Table 2.

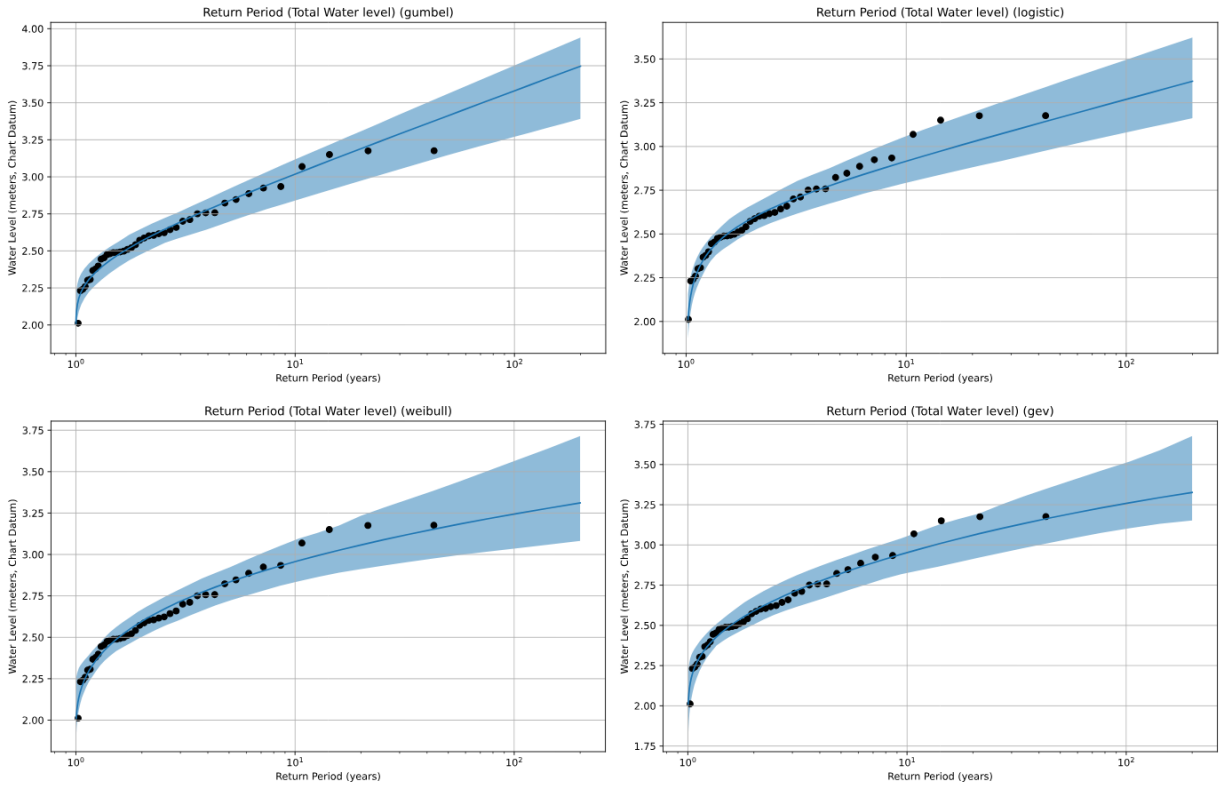

Figure 11 – Total water level return periods for Shediac Bay. The shaded regions are 95% confidence intervals generated using the bootstrap method. The black dots are empirical return periods, generated by plotting annual maxima with Weibull plotting positions as a CDF. Top left: Gumbel, top right: Logistic, bottom left: Weibull, bottom right: GEV.

Table 2 – The calculated total water level return periods in Shediac Bay for 2, 5, 10, 20, 50, 100, and 200 years using Gumbel, Weibull, Logistic, and GEV distributions.

Return Period (years)	Gumbel (metres)	Weibull (metres)	Logistic (metres)	GEV (metres)
2	2.57	2.60	2.59	2.57
5	2.84	2.83	2.80	2.82
10	3.02	2.96	2.92	2.95
20	3.19	3.06	3.02	3.06
50	3.41	3.17	3.16	3.18
100	3.58	3.24	3.27	3.26
200	3.75	3.31	3.37	3.33

Residual Return Periods

Residual (storm surge) return periods for Shediac Bay closely match the empirical return periods (Figure 12) (Table 3). Gumbel is still the preferred distribution due to having the least overestimation.

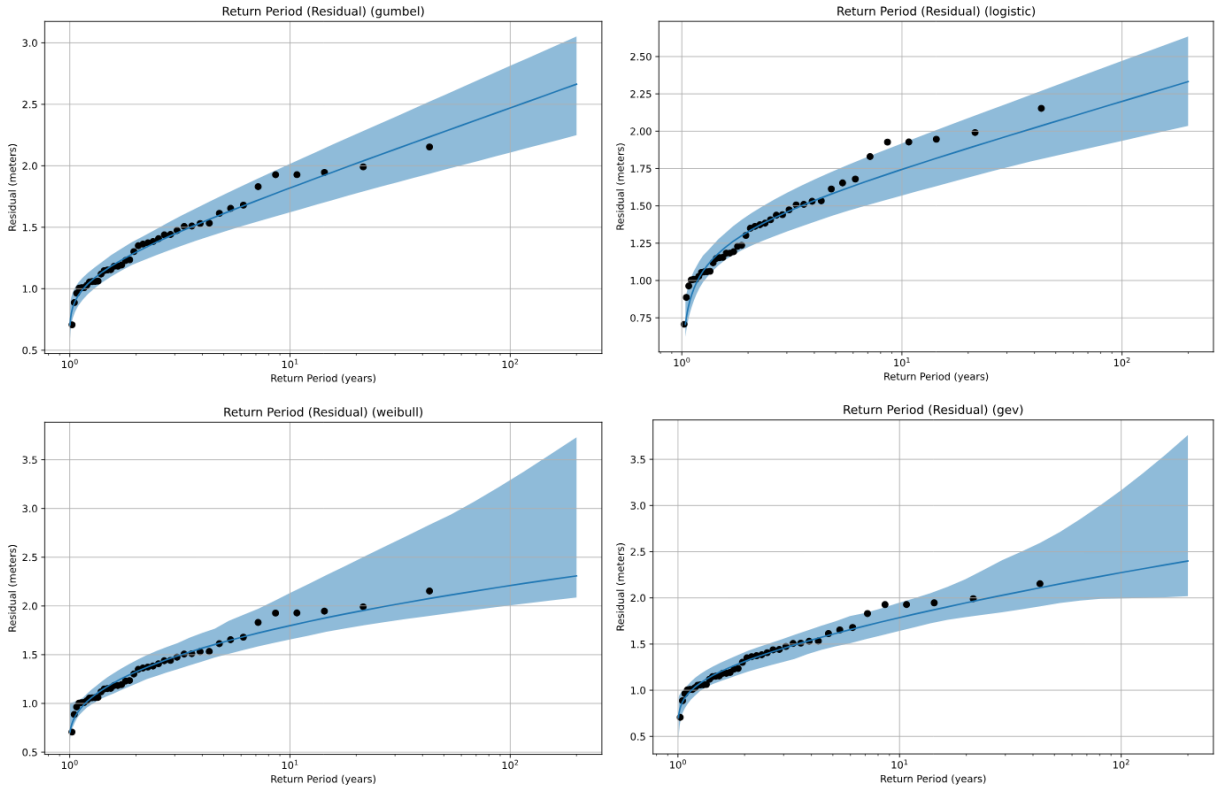

Figure 12 – Residual return periods for Shediac Bay. The shaded regions are 95% confidence intervals generated using the bootstrap method. The black dots are empirical return periods, generated by plotting annual maxima with Weibull plotting positions as a CDF. Top left: Gumbel, top right: Logistic, bottom left: Weibull, bottom right: GEV.

Table 3 – The calculated residual return periods in Shediac Bay for 2, 5, 10, 20, 50, 100, and 200 years using Gumbel, Weibull, Logistic, and GEV distributions.

Return Period (years)	Gumbel (metres)	Weibull (metres)	Logistic (metres)	GEV (metres)
2	1.30	1.32	1.33	1.31
5	1.61	1.63	1.59	1.61
10	1.82	1.80	1.74	1.79
20	2.02	1.94	1.89	1.95
50	2.28	2.10	2.07	2.14
100	2.47	2.21	2.20	2.27
200	2.67	2.31	2.33	2.40

By sorting the residual water levels, one can also calculate the empirical return periods that do not rely on a model if there are enough records. This was done for both the total water level (Table 4) and the residual water levels (Table 5)

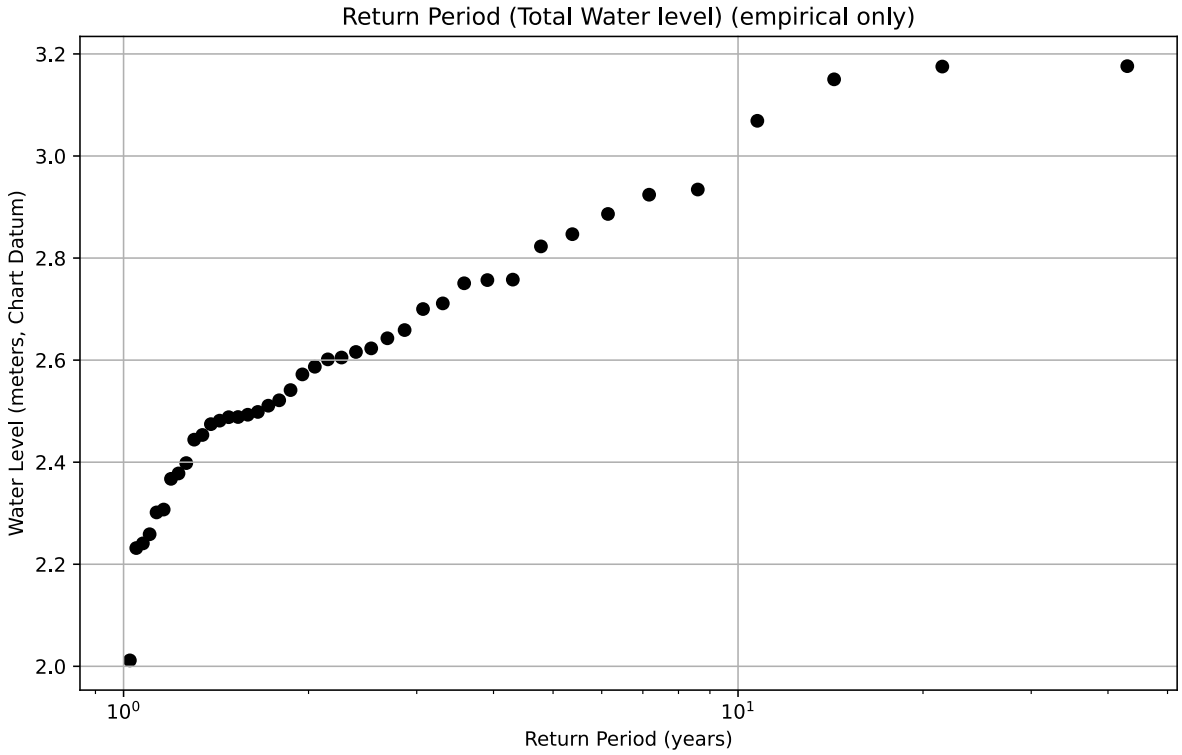

Figure 13 - Empirical total water level return periods for Shediac Bay, generated by plotting annual maxima with Weibull plotting positions as a CDF.

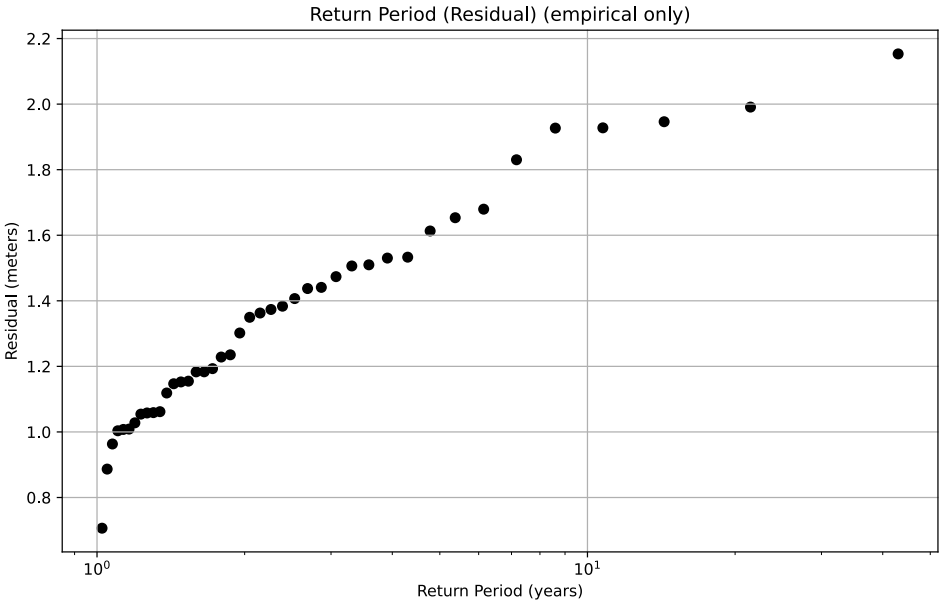

Figure 14 - Empirical residual return periods for Shediac Bay, generated by plotting residual annual maxima with Weibull plotting positions as a CDF.

Table 4 – Empirically derived 10 highest total water level records in Shediac Bay. The return periods were calculated using Weibull plotting positions.

Date	Water Level (metres)	Return Period (years)
1977-12-08 02:00	2.823	4.300
2022-01-29 23:00	2.847	4.778
1974-02-05 22:00	2.886	5.375
1988-11-21 23:00	2.924	6.143
1986-01-04 13:00	2.934	7.167
1976-03-17 18:00	3.069	8.600
2004-02-19 22:00	3.150	10.750
2004-02-19 23:00	3.150	14.333
2019-09-08 01:00	3.175	21.500
2010-12-21 22:00	3.176	43.000

Table 5 – Empirically derived 10 highest residual records in Shediac Bay. The return periods were calculated using Weibull plotting positions.

Date	Residual (metres)	Return Period (years)
1988-11-21 21:00	1.533	4.300
2018-11-29 13:00	1.613	4.778
2010-01-03 04:00	1.653	5.375
2014-03-27 02:00	1.680	6.143
2019-09-08 01:00	1.830	7.167
1977-12-08 04:00	1.927	8.600
1980-10-27 10:00	1.928	10.750
1986-01-04 13:00	1.946	14.333
1976-03-17 18:00	1.991	21.500
2004-12-28 08:00	2.153	43.000

Saint John tide gauge was processed in a similar way to show the model results for the total water level (Figure 15) and (Table 6).

Total Water Level Return Periods

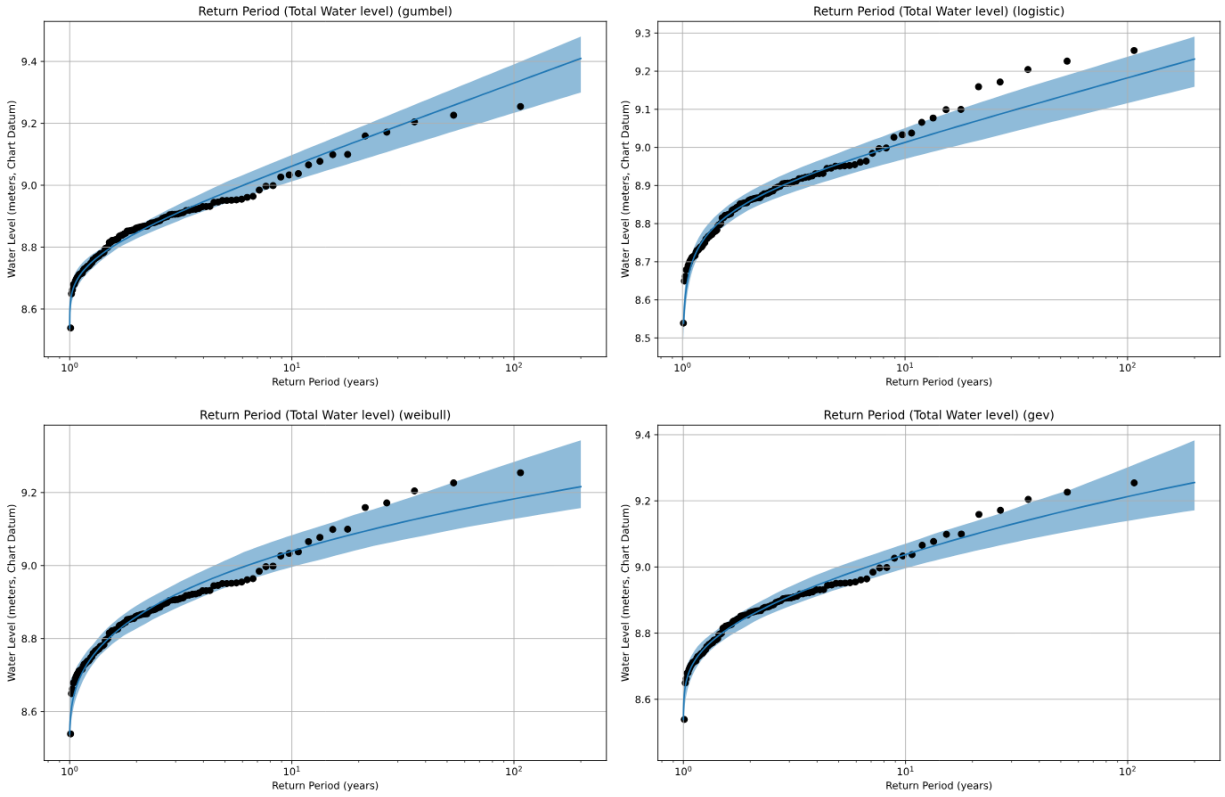

Figure 15 – Total water level return periods for Saint John. The shaded regions are 95% confidence intervals generated using the bootstrap method. The black dots are empirical return periods, generated by plotting annual maxima with Weibull plotting positions as a CDF. Top left: Gumbel, top right: Logistic, bottom left: Weibull, bottom right: GEV.

Table 6 – The calculated total water level return periods in Saint John for 2, 5, 10, 20, 50, 100, and 200 years using Gumbel, Weibull, Logistic, and GEV distributions.

Return Period (years)	Gumbel (metres)	Weibull (metres)	Logistic (metres)	GEV (metres)
2	8.846	8.86	8.86	8.85
5	8.976	8.98	8.96	8.97
10	9.061	9.04	9.01	9.03
20	9.144	9.09	9.07	9.10
50	9.250	9.15	9.13	9.17
100	9.330	9.18	9.18	9.21
200	9.410	9.22	9.23	9.26

Similarly, the Saint John tide gauge was processed to show the model results for the residual water level (Figure 16) and (Table 7).

Residual Return Periods

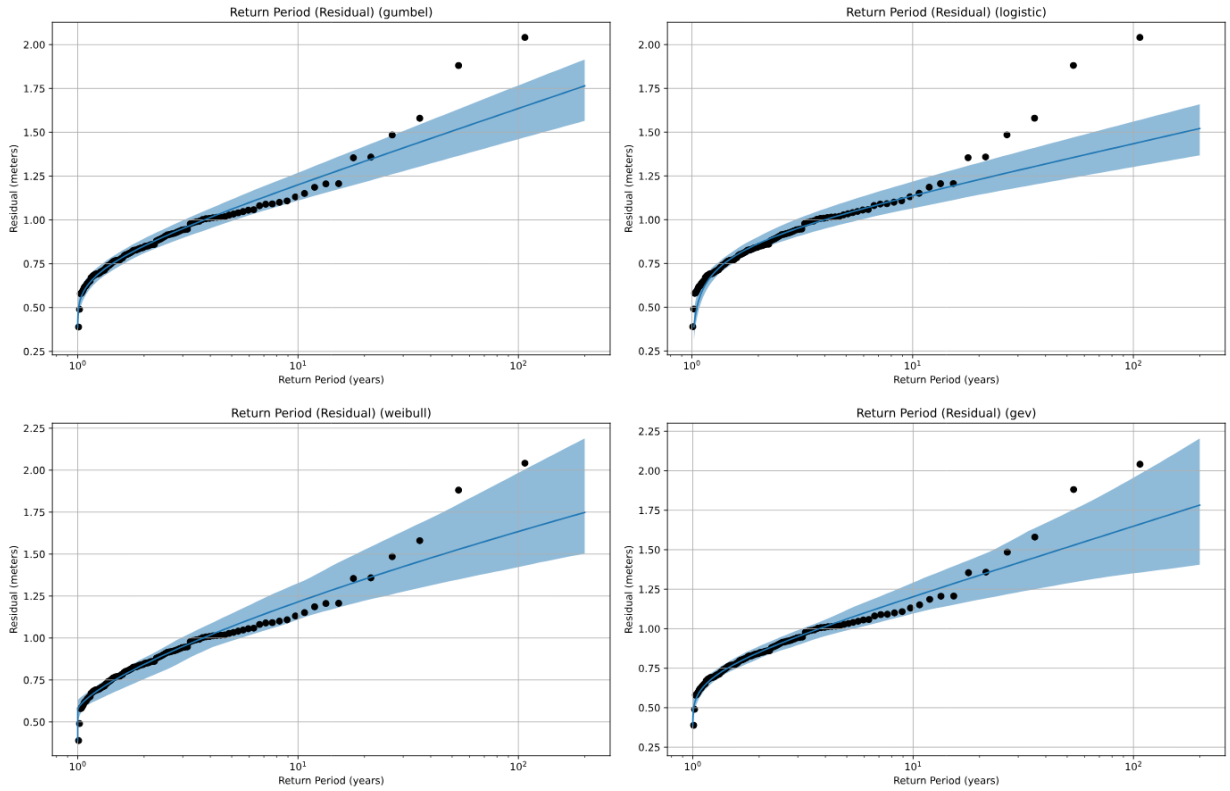

Figure 16 - Residual return periods for Saint John. The shaded regions are 95% confidence intervals generated with the bootstrap method. The black dots are empirical return periods, generated by plotting annual maxima with Weibull plotting positions as a CDF. Top left: Gumbel, top right: Logistic, bottom left: Weibull, bottom right: GEV.

Table 7 – The calculated residual return periods in Saint John for 2, 5, 10, 20, 50, 100, and 200 years using Gumbel, Weibull, Logistic, and GEV distributions.

Return Period (years)	Gumbel (metres)	Weibull (metres)	Logistic (metres)	GEV (metres)
2	0.85	0.84	0.86	0.85
5	1.06	1.07	1.04	1.06
10	1.20	1.22	1.14	1.20
20	1.33	1.35	1.23	1.34
50	1.51	1.52	1.35	1.52
100	1.64	1.63	1.43	1.65
200	1.76	1.75	1.52	1.78

The data for Saint John was also sorted and the imperially derived return periods were calculated for the total water level (Figure 17) (Table 8) and residual levels (Figure 18) (Table 9).

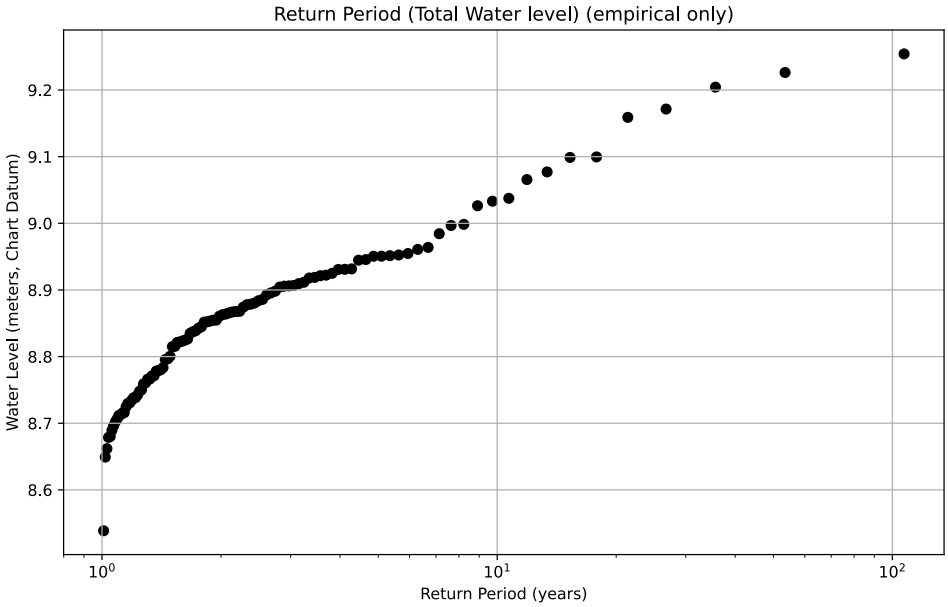

Figure 17 - Empirical total water level return periods for Saint John, generated by plotting annual maxima with Weibull plotting positions as a CDF.

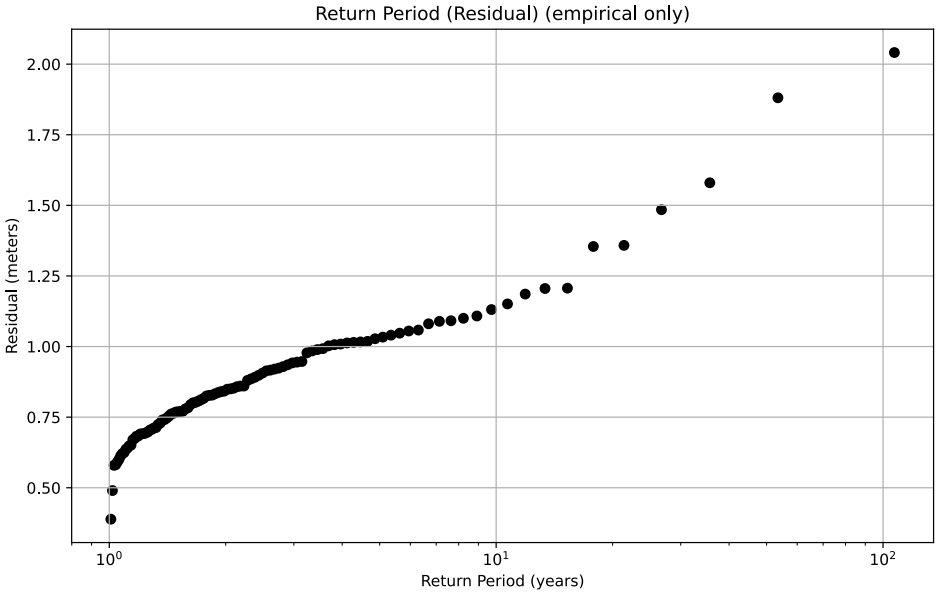

Figure 18 - Empirical residual return periods for Saint John, generated by plotting residual annual maxima with Weibull plotting positions as a CDF.

Table 8 – Empirically derived 10 highest total water level records in Saint John. The return periods were calculated using Weibull plotting positions.

Date	Water Level (metres)	Return Period
1916-01-05 15:00	9.038	10.700
1979-09-07 04:00	9.066	11.889
1924-07-18 04:00	9.077	13.375
2020-04-10 05:00	9.099	15.286
1978-01-09 15:00	9.010	17.833
1953-02-16 05:00	9.159	21.400
1977-04-06 05:00	9.171	26.750
1997-01-10 16:00	9.204	35.667
1945-11-20 16:00	9.226	53.500
1976-02-02 17:00	9.254	107.000

Table 9 – Empirically derived 10 highest residual records in Saint John. The return periods were calculated using Weibull plotting positions.

Date	Residual (metres)	Return Period
1946-01-14 19:00	1.151	10.700
1967-11-25 01:00	1.186	11.889
1983-12-07 09:00	1.206	13.375
1971-04-22 21:00	1.207	15.286
1954-09-12 00:00	1.354	17.833
1976-02-02 17:00	1.358	21.400
1955-05-24 02:00	1.485	26.750
1951-12-05 00:00	1.580	35.667
1956-12-27 16:00	1.881	53.500
1950-02-25 00:00	2.041	107.000

2.4 Logger Site Selection and Deployment Methods

To find a suitable location to deploy the water level logger, NSCC-AGRG and MCC staff discussed potential sites in MCC along the coast of the Northumberland Strait (Figure 19). It is important to be able to attach the water level logger to a sturdy, permanent structure that won't move with the tide. Wharves are often the best candidates. A wharf in Northport that appeared suitable was selected (Figure 20). Permission was obtained from the Harbour Authority of Northport to attach the sensor setup to the wharf in Northport selected by the group and plans were made by NSCC-AGRG and MCC staff to visit the site at low tide for the installation.

An Onset Titanium HOBO Water Level Logger (WLL) was initially handed off by NSCC-AGRG to MCC staff to collect data to calculate a time series of water levels at the deployment site. The model of logger used in this project is meant to be deployed where water above the sensor is expected to reach from 0 to 9 meters. The precision of the readings for this model is rated at a 2.1-millimeter resolution. It is more precise than the loggers rated for use in deeper water. The titanium loggers are lighter than the standard loggers and generally better suited for coastal use compared to the standard steel loggers, which are more prone to corrosion and damage in these challenging coastal areas. However, these loggers are still not impervious to damage as will be discussed in the sections to follow. Logger data collected is referenced to UTC.

Figure 19 An Onset HOBO U20 Water Level Logger. This is a standard model meant for water up to 9 metres above the sensor eye. The sensor eye where the water pressure is measured and the cap covering the communication port are marked for reference. The titanium models are nearly identical in appearance, aside from the markings identifying them as being titanium.

NSCC-AGRG's water level logger deployment setup for this project is as follows. One large board gets attached to the structure on site (wharf) with a PVC pipe that the logger is deployed in (Figure 20). The logger hangs a known distance of steel line down from the top of the pipe attached to a PVC cap. An additional nylon rope is connected to the logger to the cap for extra security in the event that the steel line breaks or wears out. This rope does not set the distance of the sensor from the cap. This setup is

sturdy and suitable for long-term deployments and allows for easy checkup on sensors as needed to download data and verify regular function.

Figure 20 Former AGRG colleague Lucas Mackay on the day of deployment, pictured with the logger deployment structure.

The final step of logger deployment is to take the measurements needed to reference the logger's sensor eye to an elevation in CGVD2013. With a survey-grade GNSS unit, a point is collected where the position will be the most accurate (Figure 22). This requires the GNSS antenna's view of the sky not be obstructed. The deck or edge of the wharf above where the logger is attached to is generally where the point is collected. Next, measurements are taken with a tape measure to relate the sensor eye to the point taken with the GNSS unit. In the office, a diagram is created (Figure 21), and the math is done with the work shown to determine the elevation of the sensor eye. When possible, the GNSS system is also used to collect points at the water's edge for water levels to validate the water levels derived from the logger.

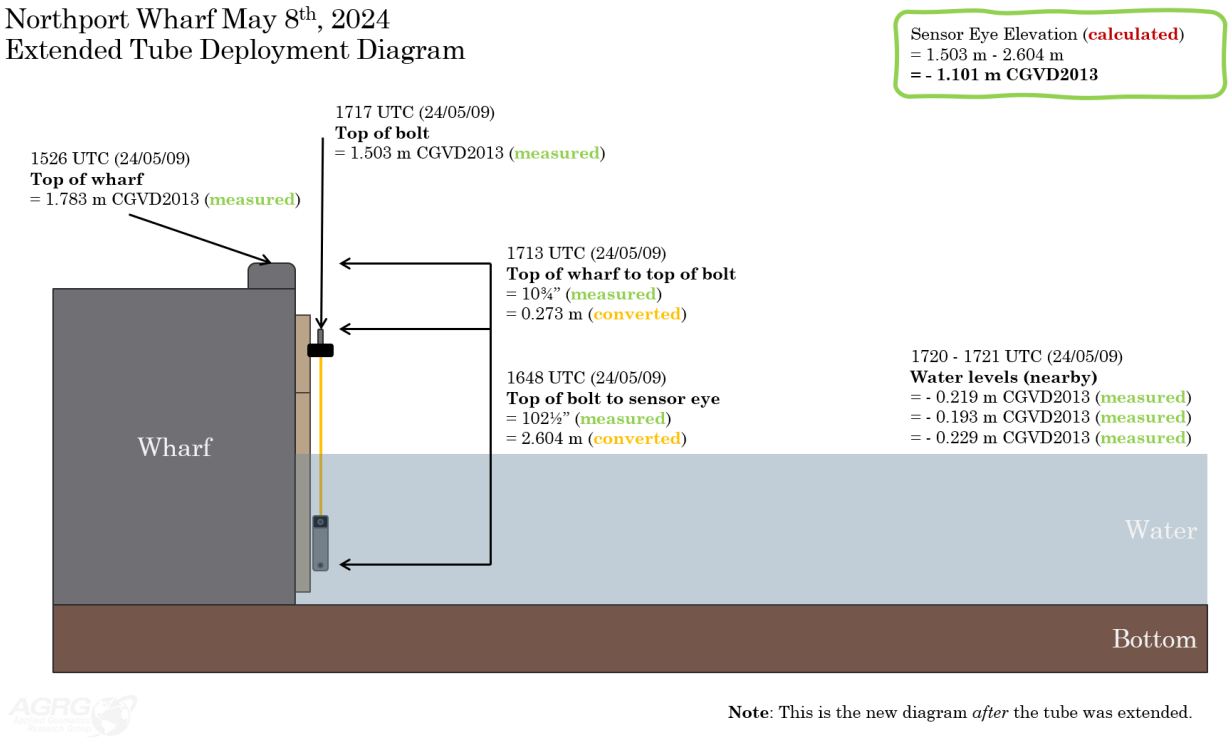

Figure 21 Example deployment diagram for the Northport logger.

Figure 22 Colleague Sean Dzafovic collecting the GNSS reference point for the Northport Wharf.

Logger Data Processing Methods

The data collected by HOBO Water Level Loggers require processing after being retrieved and downloaded to be converted to water level elevations. The loggers record water pressure exerted by the water above the sensor at the sensor eye, which itself is converted from the voltages returned by the sensor in the logger based on the unit's calibration in Onset's HOBOware software, and thus do not record water levels directly. The height of the water above the sensor is calculated by using the hydrostatic water pressure formula, $P = \rho * g * h$, where

P is pressure of a fluid at depth

ρ is the density of saltwater

g is the acceleration of gravity

h is the height of the water column

After rearranging the formula to solve for height of the water column, we need to use the atmospheric pressure for the area to subtract from the water level logger's pressure readings to get the pressure exerted by just the water column above the sensor. NSCC-AGRG typically uses historical atmospheric pressure data for a given site, either from the nearest Environment Canada-run weather station or using data accessed from their Meteomatics weather API subscription. From here, the data gets processed using cell equations in an Excel spreadsheet.

The final step of processing the data adds the height of the sensor eye in CGVD2013 as determined by the reference measurements collected in the field. Validation water levels are compared to water levels from the logger where available for data quality assurance. Adjustments may be made to the logger water levels to better match the trusted validation water levels when appropriate.

Deployment Location Results and Discussion

NSCC-AGRG determined that the most suitable site for deployment of this logger was at a wharf in Northport run by the Harbour Authority of Northport (Figure 23, Figure 24). After getting permission to install the logger to the wharf, NSCC-AGRG colleagues Tim Webster, Sean Dzafovic, and Lucas Mackay went with MCC staff on September 22nd, 2023 to install the logger setup. The logger deployed at this time belonged to NSCC-AGRG, as the sensor ordered for MCC had not arrived yet.

Figure 23 Overview of the Northport water level logger's deployment location.

Figure 24 Aerial view of the wharf in Northport where the sensor was installed, taken May 8th, 2024. The location of the logger on the wharf is outlined for the viewer.

After deploying the logger, the group decided the logger board and pipe install were too short. The initial install was too low to be able to retrieve the data from the wharf deck at high tide and required a visit at low tide and access via the ladder next to the logger. NSCC-AGRG made plans to meet up with the MCC staff team again in the spring of the following year to extend the pipe for easier access and to swap NSCC-AGRG's logger for the MCC's logger after it arrived. On May 8th, 2024, NSCC-AGRG colleagues Sean Dzafovic and Thomas Allen returned to the wharf and met with MCC staff to install the extension to the deployment as seen in Figure 25. After this point, the logger was able to be accessed from the wharf deck regardless of tidal cycle. NSCC-AGRG also downloaded the data from the logger and showed MCC staff how to download data, maintain the logger, and handed off the instructional materials to MCC staff showing how to operate the logger and process the data on their own. NSCC-AGRG deployed the new logger purchased on behalf of the MCC in the newly extended setup and returned to their office in Middleton with their original sensor.

Figure 25 Logger deployment setup on May 8th, 2024. This photo was taken after the extension to the tube was added.

Issues With Loggers – Malfunctions

After the first revisit to the site in May 2024 and processing the data, it was discovered that the logger malfunctioned over the winter, likely due to sea ice damaging it. The first spike in the data was seen in January, after sea ice was present (Figure 26). When these loggers get iced over, the pressure they are subjected to is much higher than that of the usual volume of water, thus the processed water elevation reached 8 metres CGVD2013 for the first spike. Luckily, this data is easy to identify and manually remove from the valid data by looking for the pressure readings that dramatically exceed what is

expected. This area does not typically get a 6m surge, so a reading of 8 m CGVD2013 can be considered erroneous. A second icing-over event was recorded in March of 2024, after which all the recorded data stored by the logger became unusable. This failure was not catastrophic, but it required the logger to be sent to Hoskin Scientific for servicing. Fortunately, this malfunctioning logger belonging to NSCC-AGRG was swapped out for the brand-new logger purchased for MCC on the revisit in May.

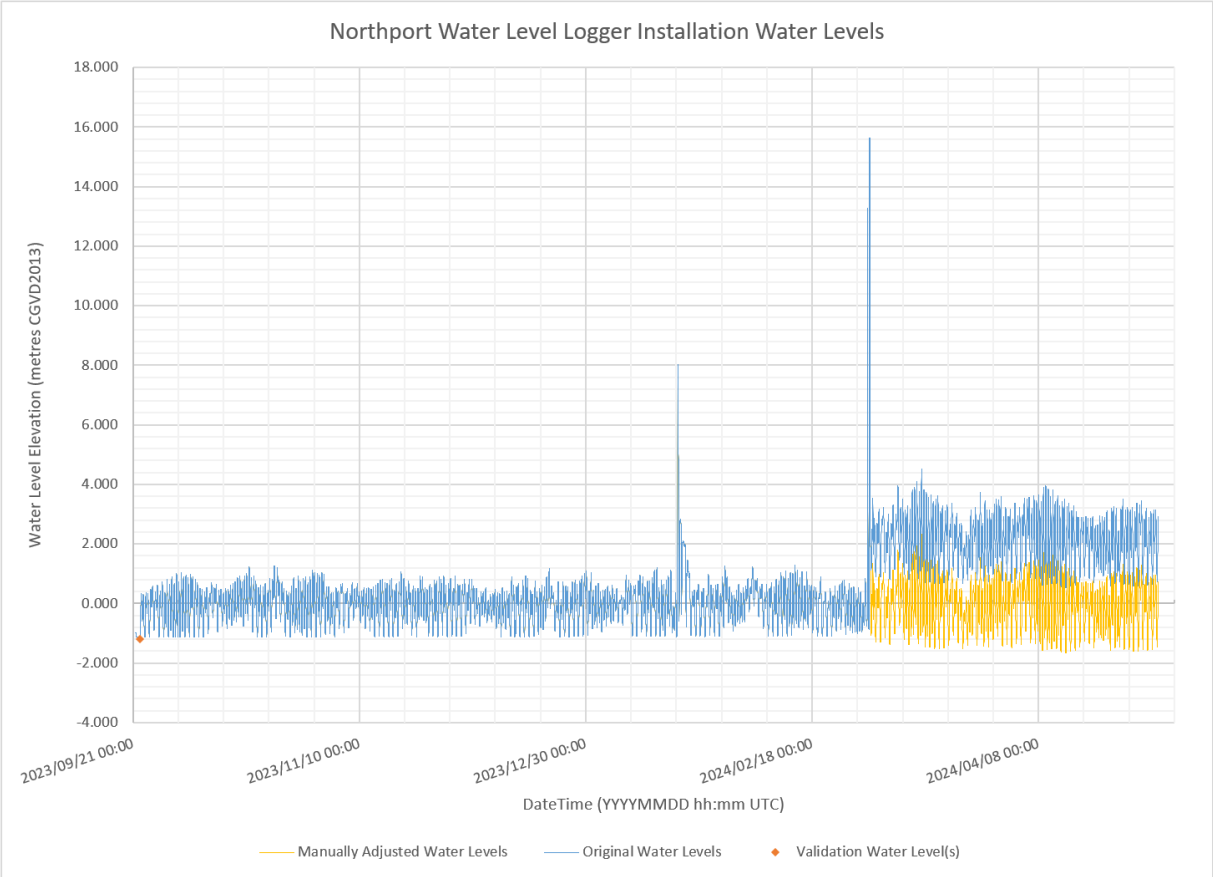

Figure 26 Plot of the data from the original deployment, processed by AGRG after being downloaded on the May 2024 visit. The blue line represents the unmodified pressure data after being processed into water level elevations. The yellow line represents the data after the second ice event shifted down to meet the good water level. We can see that even after shifting the bad data down to meet the good data, the amplitude is off, and the data is unusable.

Unfortunately, the MCC logger eventually malfunctioned as well, suffering more damage than the previous logger. In correspondence with NSCC-AGRG in the summer of 2025, MCC staff noted that they could not read the logger on their last visit in May of 2025 after having successfully read the logger in September of 2024. In June, MCC staff sent a photo (Figure 27) confirming that the logger had sustained damage as seen by the water in the unit where the logger communicates with the shuttle interface plugged into the computer. NSCC-AGRG met with MCC staff to exchange loggers in July 2025. NSCC-AGRG

loaned MCC staff another of their sensors to use while they sent the MCC logger to Hoskin Scientific for data recovery and servicing. In October of 2025, Hoskin Scientific sent NSCC-AGRG the data recovered from the logger, allowing for the logger's failure to be investigated further. Interestingly, the logger's pressure sensor failed at the end of September 2024, rather than during the winter when issues are to be expected (Figure 28). The logger's temperature sensor continued to work until the entire logger stopped working in December 2024, after logging a bad battery warning in November 2024.

The logger loaned to MCC staff in July did not get deployed before MCC's own logger returned from servicing. NSCC-AGRG colleague Sean Dzafovic met with MCC staff in January 2026 to hand off MCC's repaired logger and take NSCC-AGRG's loaned logger back. As of March 2026, this logger has not been re-deployed and the Northport site's PVC pipe install is empty.

Figure 27 Damaged MCC logger, as seen in email correspondence with Maggie Pitts in July 2025.

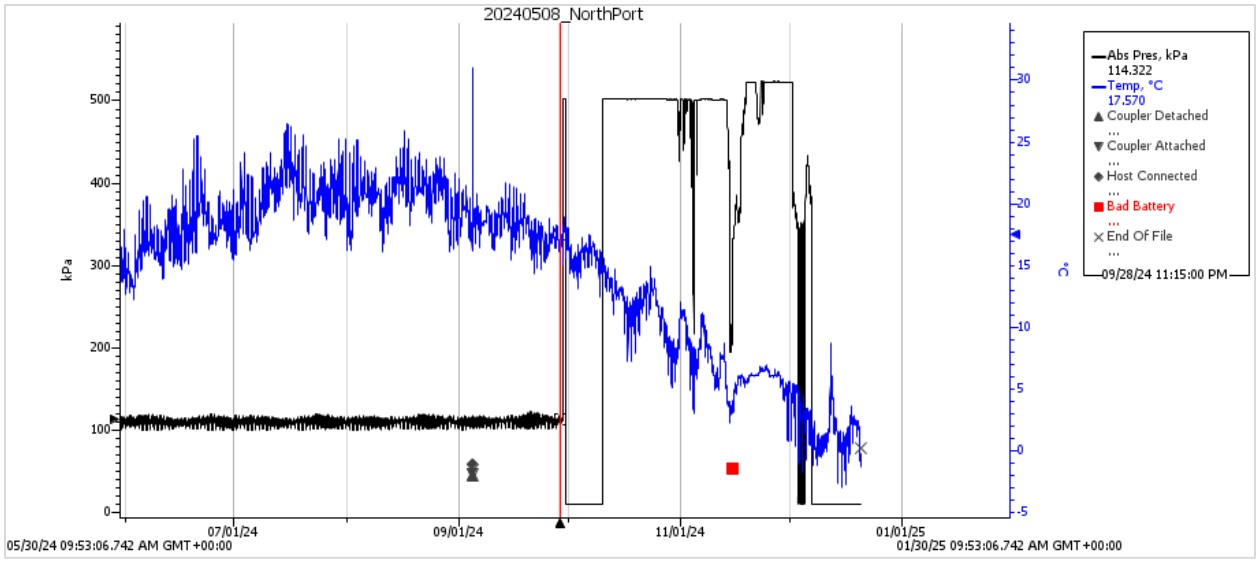

Figure 28 View of the MCC logger data from within the HOBOware software. Note the pressure sensor failure in September 2024. The temperature sensor continued to work until the logger stopped working completely in December 2024.

Current Status

After cleaning the data and removing data from logger malfunctions, we have two records of water levels for the Northport site that last from September 22nd, 2023 to March 1st, 2024 and May 8th, 2024 to September 29th, 2024. Additionally, we have acquired XTide-based predicted tides from nearby Tidnish and Pugwash stations that can be seen in *Figure 30* and *Figure 32*, as well as *Figure 33* where the plot is focused on a smaller sub-section of data for the viewer to better see the relationship between the different data sources. Residuals for the two records were calculated by subtracting the observed tide from the predicted. Note that we can see in these plots that the very lowest tides do not get recorded by the Northport logger, as the logger becomes exposed to the air and is no longer submerged when the water level goes just below -1 m CGVD2013 in elevation. These data points were excluded from calculations of storm surge/residuals.

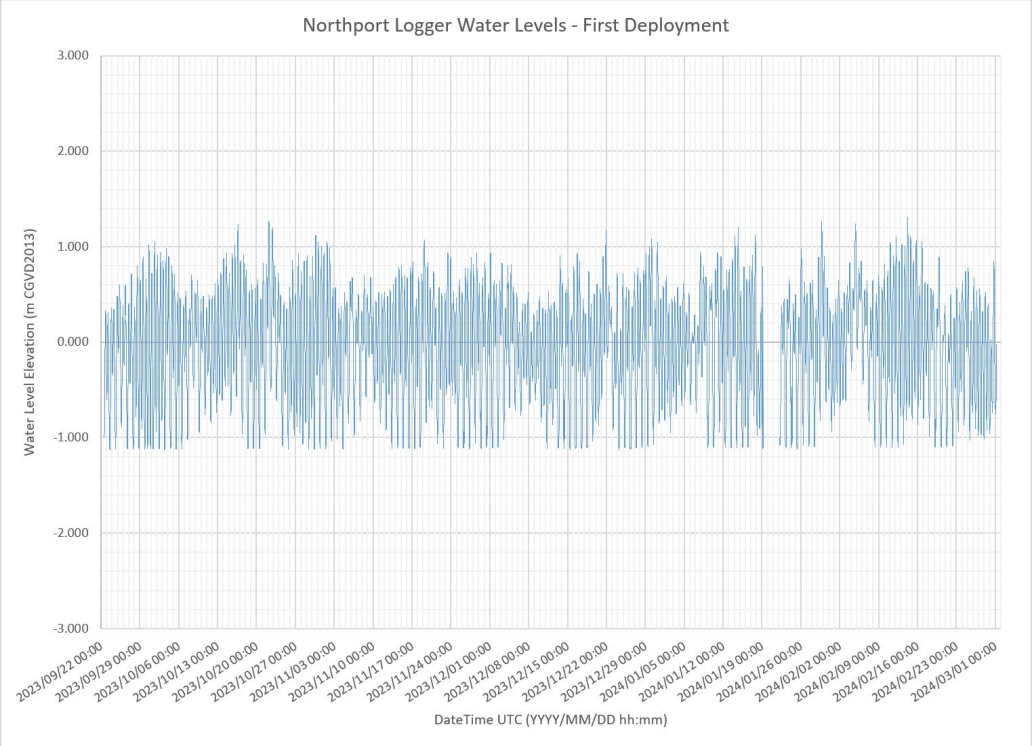

Figure 29 Full record of the first logger deployment with bad data from ice and logger failure cut out, processed to water levels referenced to the CGVD2013 vertical datum.

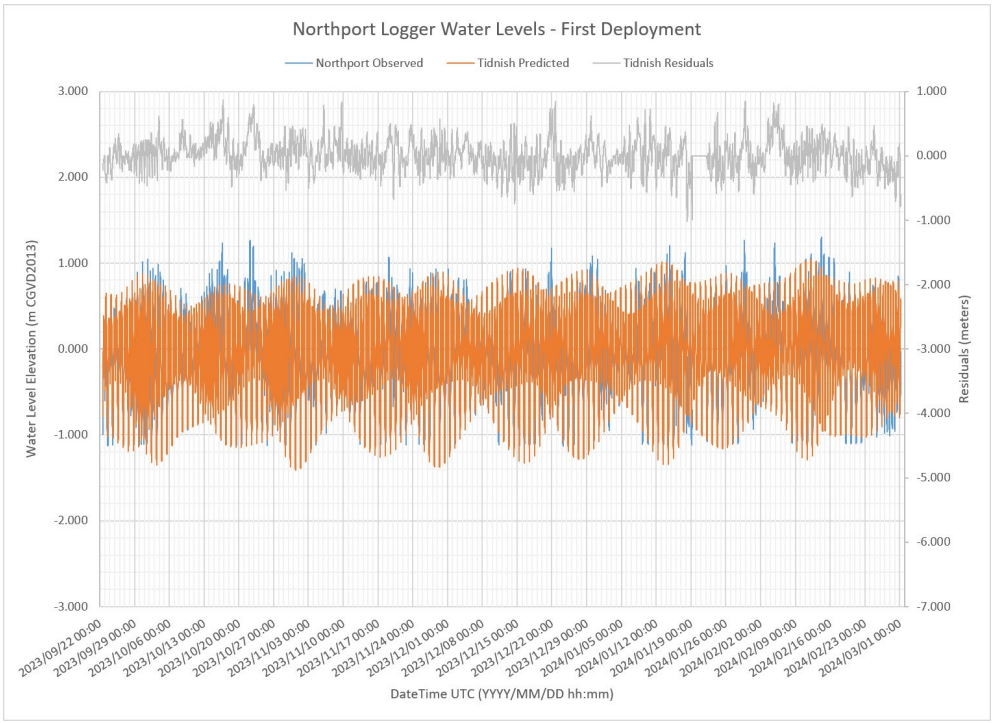

Figure 30 Full record of the first logger deployment with bad data from ice and logger failure cut out, processed to water levels referenced to the CGVD2013 vertical datum and including predicted tide levels for nearby Tidnish Xtide station and calculated residuals.

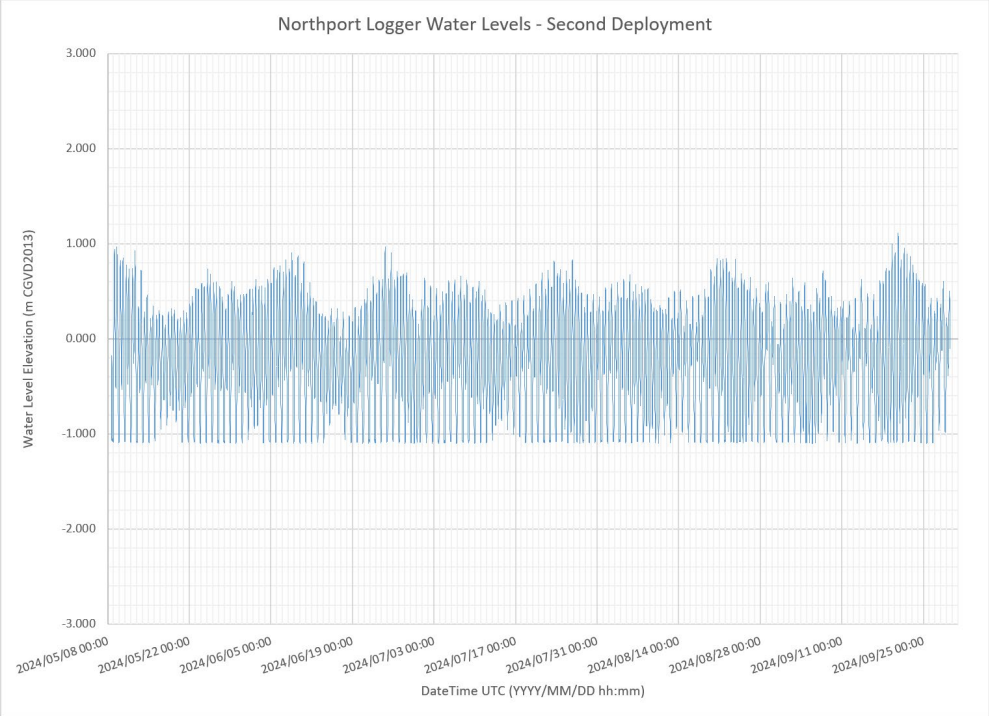

Figure 31 Full record of the second logger deployment after the failure of the original logger, processed to water levels referenced to the CGVD2013 vertical datum.

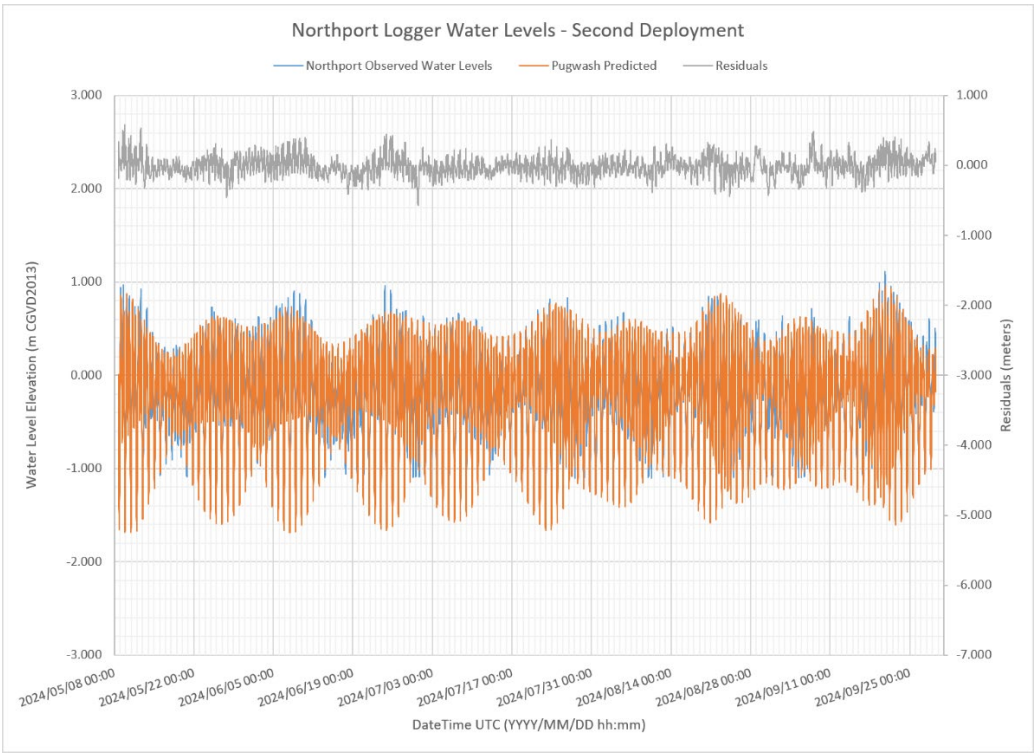

Figure 32 Full record of the second logger deployment after the failure of the original logger, processed to water levels referenced to the CGVD2013 vertical datum and including predicted tide levels for nearby Pugwash Xtide station and calculated residuals.

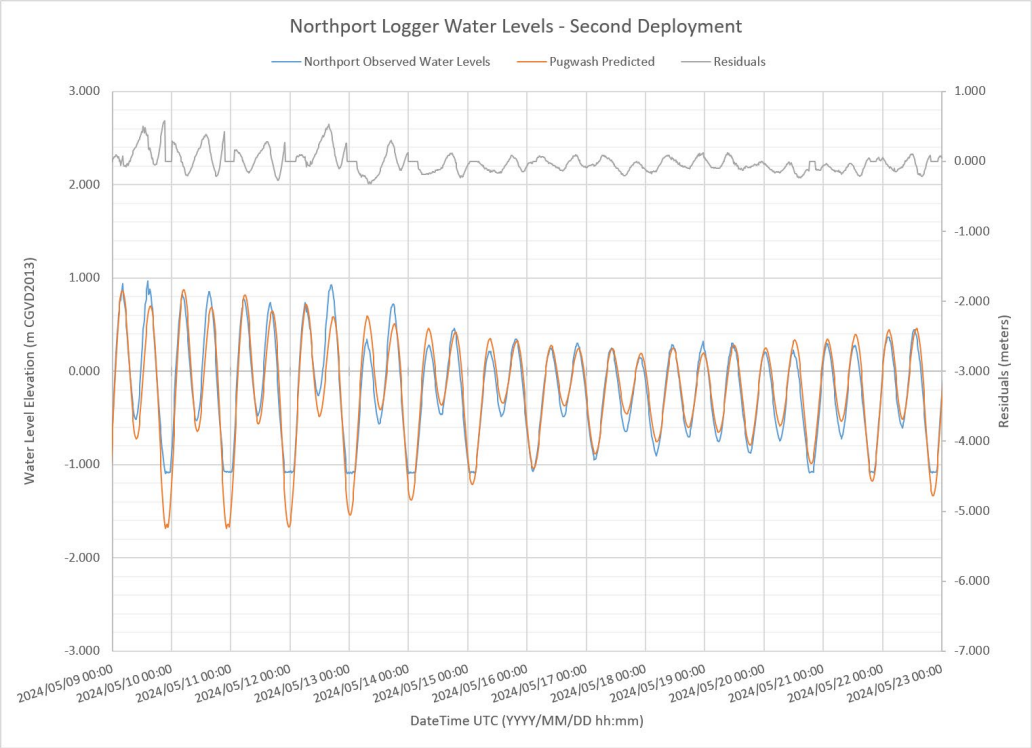

Figure 33 A two-week selection of data from the second Northport deployment for an easier to interpret example for the reader.

NSCC-AGRG is currently investigating potential replacement sites for this logger for MCC staff. The current rate of failure of sensors at the Northport site is not acceptable and indicates an issue with the site itself. If this logger is to be installed permanently year-round, a site where the logger is deployed deep enough to not be frozen over the winter is needed. Currently, the logger is exposed at the lowest tide levels. On a revisit in the summer of 2026, the depths of other points along the Northport wharf were measured, but none were found that NSCC-AGRG believed to be deep enough to fix current freezing issues. Further investigation is needed.

HOBO 0 to 9 meter Water Level Logger Specifications (HOBO U20-001-01 and U20-001-01-Ti)

https://www.onsetcomp.com/products/data-loggers/u20-001-01#specifications

HOBO 0 to 30.6 meter Water Level Logger Specifications (U20-001-02 and U20-001-02-Ti)

https://www.onsetcomp.com/products/data-loggers/u20-001-02#specifications

Website providing xtide-based predicted tides used in this project

https://tide.arthroinfo.org/

3 Results

3.1 Static Flood Layers

The hydro-connected DEM was used to generate flood inundation layers every 10 cm from 0 m to 15 m CGVD2013 for both the Northumberland and the Fundy coasts. The vector flood inundation polygons are labelled Flood_0_0m through to Flood_5_5m to Flood_15_0m which translates into the flood level at 0.0 m, 5.5 m and 15.0 m CGVD2013 for each coast the MCC.

After Hurricane Fiona made landfall Sept. 24, 2022, NSCC-AGRG sent crews out with drones to capture the high-water marks and then used the provincial lidar to estimate the elevations. On the Northumberland coast of the MCC the elevations of the high-water marks ranged from 1.2 – 2.9 m CGVD2013. Heather Beach Provincial Park was surveyed with the drone and then the water raised to match the wrack line to an estimated value of 2.9 m. Thus the 10 cm flood layers can be used to examine the potential impacts of another storm like Fiona (Figure 34).

Figure 34 Top map is a drone ortho mosaic showing the debris line near parking lot at Heather beach. The bottom map shows a water level of 2.9 m CGVD2013, flood layer Flood_2_9m.

3.2 Return Periods

The provincial coastal flood guidelines call for using the water level associated with the 1 in 20-year and 1 in 100-year storm surge events. This water level (20-year or 100-year) is then added to the Higher High water Large Tide (HHWLT) value, typically the average highest tides to occur in a 19-year tidal cycle.

There are generally two main sources of calculating return periods of total water level or water level residual (storm surges): 1) Directly from tide gauge observations, and 2) From hindcasts where storm surges are simulated going back 40-65 years and then the resultant water levels are used to conduct Extreme Value Analysis to calculate the return periods.

In the previous section we described how the tide gauge data were processed and the empirical return periods obtained for both the total water level and for the residual storm surge levels. We also described and reported on using several extreme value models (Gumbel, Weibel, etc.) to calculate specific return periods, for example the 20-year and 100-year, based on a model fitted to the extreme values. More examples are presented in Appendix 1 Return Period Tables & Tidal Charts.

During Atlantic Climate Adaptation Solutions project in the 2009-12 period the province hired Richards and Daigle (2011) to compile coastal water level residual return periods and climate change projections. Richards and Daigle (2011) relied on a PhD thesis by Bernier (2005) who used 6-hr wind data to simulate storm surges for a 40 year hindcast and from those data calculate the return period for storm surges. As pointed out by Webster et al. (2012) and Bernier (2005) the fact that the model was driven by 6 hr time step for the wind means the model did not resolve short lived events like hurricanes where the water level could rise quickly and then recede as the event passed. Thus, the Bernier (2005) model produced return period water levels that were underrepresented because of this limitation in the model (i.e. 6 hr winds). Subsequent to this, Zhang and Sheng (2013) produced a similar model for the entire western Atlantic coast and generated grids representing the 50-year and 100-year storm surge return periods. However, they used the same 6 hr wind and pressure fields to drive their storm surge model. Thus, it suffered from the same issue as Bernier (2005) for not being able to resolve short lived events like hurricanes. To test their model, they compared their results of return period water level from the model to actual tide gauge records. To compensate for the 6-hour model, they filtered the tide gauge data using a low-pass (averaging) filter which smoothed over the short-lived high-water events and compared the filtered observations with their model and achieved an RMSE of 30 cm. Thus, their model grids are considered to be underestimates as well. For example, the 50-year storm surge (residual) return period calculated from the Charlottetown tide gauge was ~1.55 m while the filtered value was reduced to ~1.25 m which agreed more closely with their model result (Figure 35).

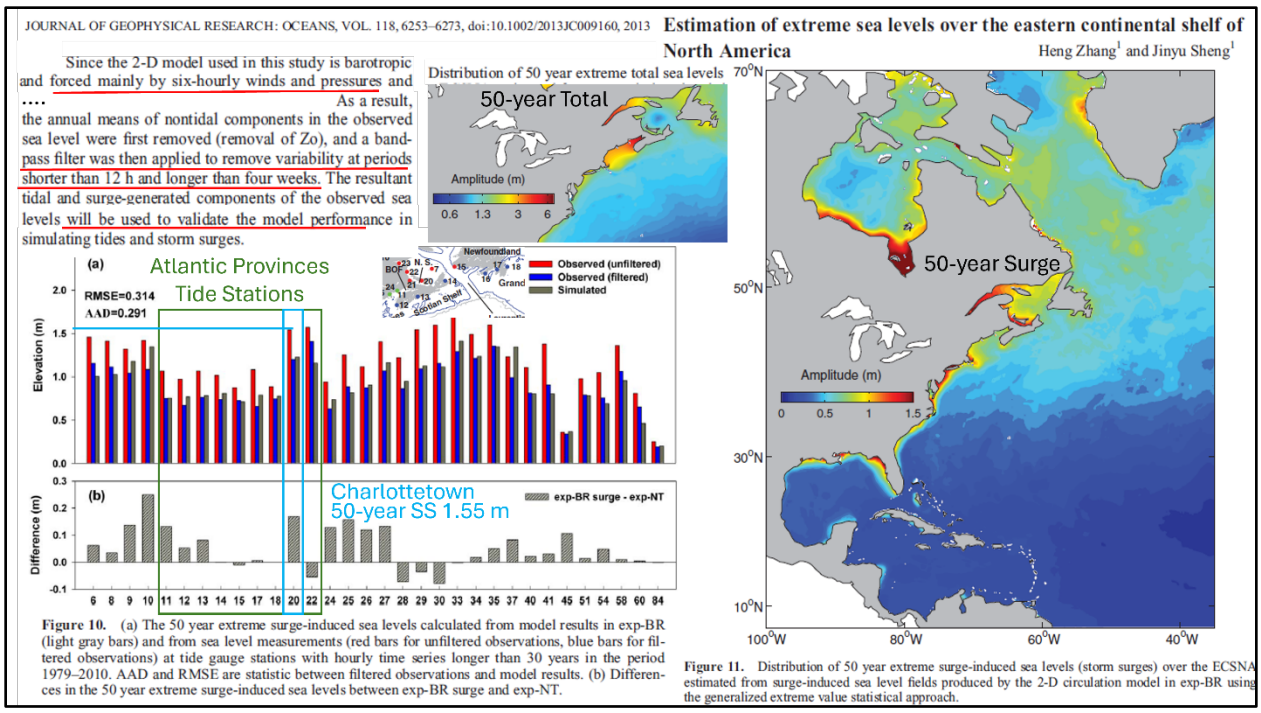

Figure 35 Summary of Zhang and Sheng (2013) paper where they modelled the 1 in 50 and 1 in 100-year storm surge return periods from a hindcast.

More recently Wang and Bernier (2025) produced a 65-year hindcast using hourly wind and pressure for the entire world coastline. They produced a series of points along the coastline at roughly 6 km spacing where they report the residual water level for the modelled 50 and 100-year events using a Gumbel extreme value distribution. When our empirical and extreme value model results are compared with Wang and Bernier (2025) and Zhang and Sheng (2013), our results are always higher (Table 10).

Table 10 Comparison of tide gauge (empirical and model) and hindcast models (Wang & Bernier (2025) and Zhang & Sheng (2013)).

Station Name	20 year Empirical	50 year Empirical	100 year Empirical	20 year Gumbel Model	50 year Gumbel Model	100 year Gumbel Model	Wang and Bernier 50 year Gumbel	Wang and Bernier 100 year Gumbel	Zhang and Sheng 50 year unfiltered	Zhang and Sheng 100 year unfiltered
Saint John	1.36	1.88	2.04	1.33	1.51	1.64	1.01	1.09	0.78	0.83
Charlottetown	1.46	1.58	1.76	1.45	1.62	1.74	1.4	1.5	1.23	1.33
Shediac Bay	1.99	(43-year) 2.15	(43-year) 2.15	2.02	2.28	2.47	2.05	2.23	1.43	1.48

Of these various return periods along with previous estimates by Richards and Daigle (2011) we have extracted the 20-year and 100-year return period using the NS Floodline guidelines for the Northumberland and Fundy coasts (Table 11).

3.3 Coastal Flood Hazard Maps

Table 11 Water levels (CGVD2013) used for the 1-20 and 1-100-year coastal flood hazard for Northumberland and Fundy coasts.

	20-year TOTAL m CGVD2013	20-yr RSL 2050	20-yr RSL 2100	20-yr Antarctica sheet 2100	100-year TOTAL m CGVD2013	100-yr RSL 2050	100-yr RSL 2100	100-yr Antarctica sheet 2100
	20-year	100-year	20-year 2050	100-year 2050	20-year 2100	100-year 2100	20-year 2100 + AA	100-year 2100 + AA
Northumberland	2.66	2.96	3.1	3.4	3.9	4.2	4.55	4.85
Fundy	15.55	18.23	15.98	19.09	16.78	20.29	17.43	21.99

The flood hazard layers were constructed for these return periods and timeframes using the bathtub model and RSL projections produced by James & Brierley Green (in prep) from the Intergovernmental Panel on Climate Change (IPCC) AR6 sea level rise scenarios, based on Shared Socioeconomic Pathways (SSPs). NSCC-AGRG used the medium confidence AR6 SSP5-8.5 RSL layers (83rd percentile), representing a very high emissions pathway. Here, "medium confidence" is an IPCC qualitative assessment that reflects moderate agreement among experts and moderate lines of evidence, while the "83rd percentile" refers to a quantitative exceedance probability that captures the upper-range values within the projection distribution. We compared the RSL grids produced by James et al. (2021) that used the AR5 RCP values to the AR6 SSP values to determine how different they are. The medium confidence RSL values using AR6 SSP5-8.5 (83rd percentile) projections are in close agreement with the AR5 RCP 8.5 projections at the 95th percentile (upper confidence) in 2050 but show higher sea levels by 2100 and 2150. In the years 2100 and 2150, the RSL is higher in the latest AR6 projections than the previous AR5 report. For the 2100 layer we also added the recommended 65 cm to the RSL project for the potential on the western Antarctica ice sheet collapse.

Examples of the coastal flood layers for Northumberland and Fundy are provided respectively (Figure 36, Figure 37).

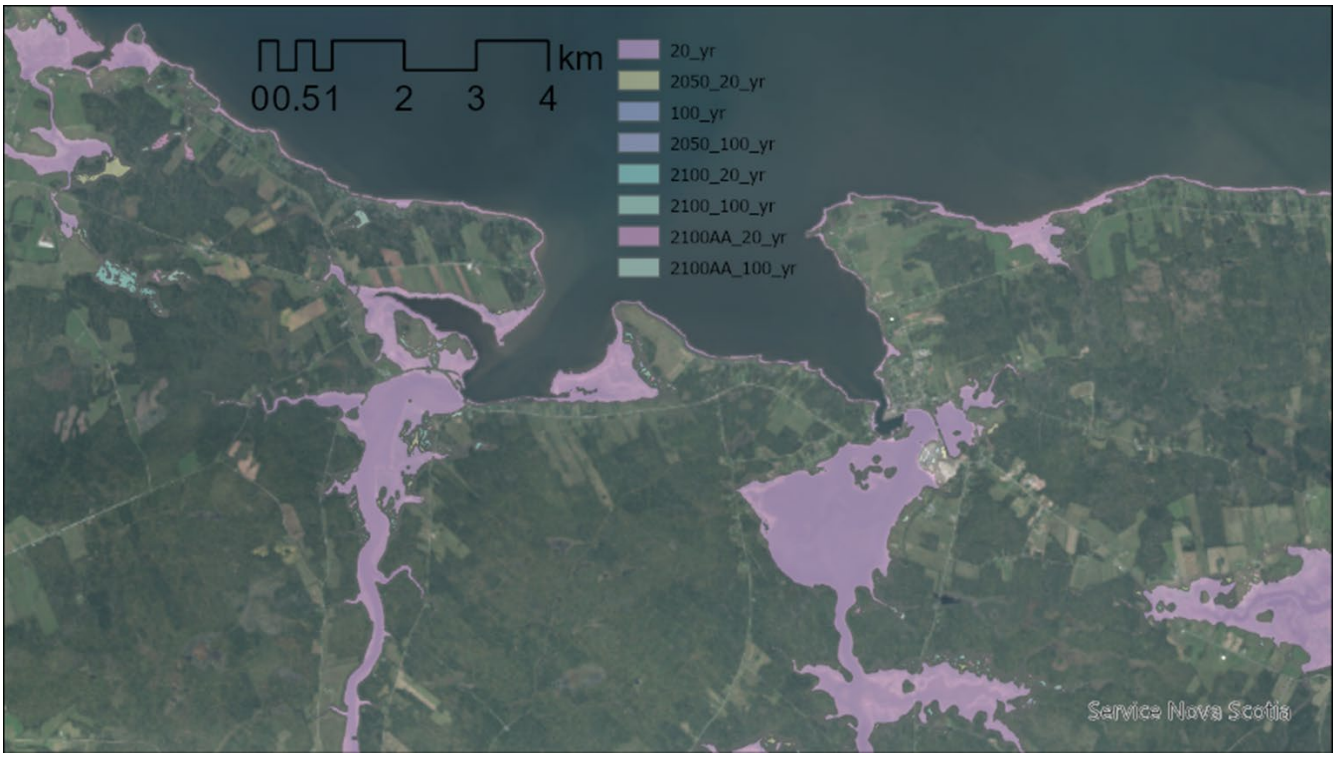

Figure 36 Example of coastal flood hazard layers near Pugwash on the Northumberland Strait for 1-20 and 1-100-year events today and in 2050 and 2100.

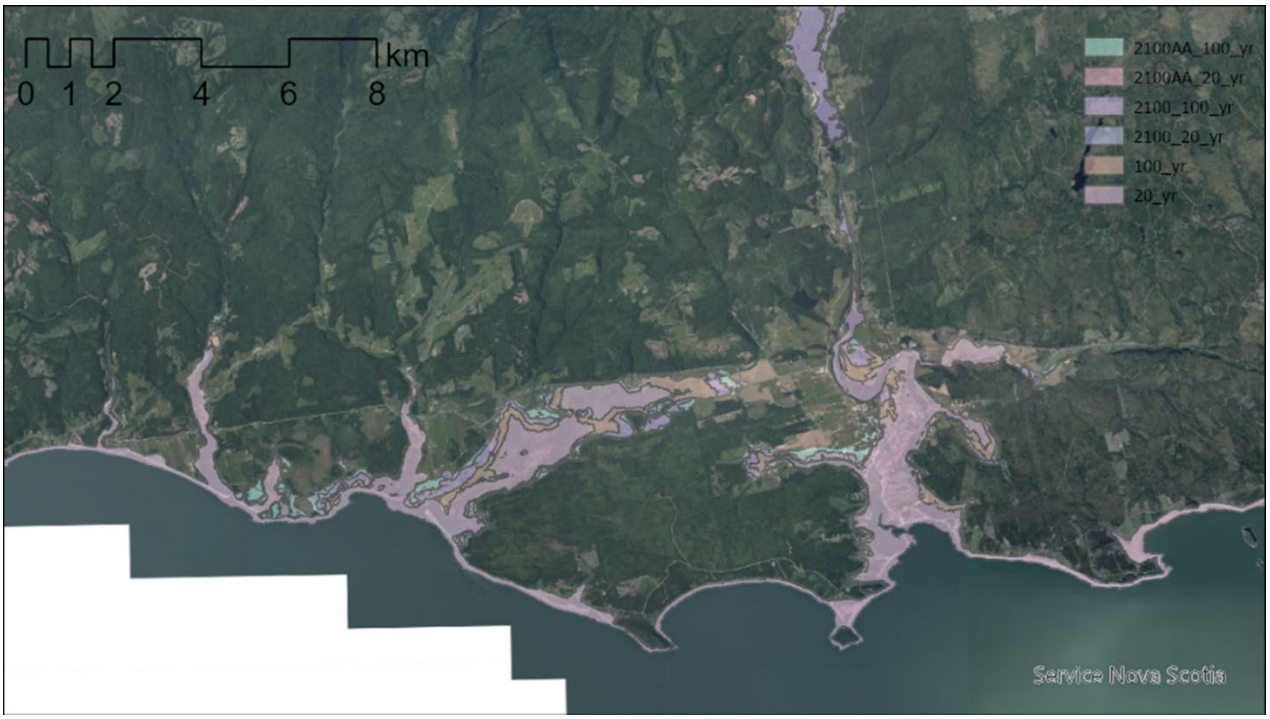

Figure 37 Example of coastal flood hazard layers near Parrsboro on the Bay of Fundy for 1-20 and 1-100-year events today and in 2050 and 2100.

It should be noted that adding the storm surge water levels to HHWLT immediately overtops the dykes in the Amherst region.

4 Conclusion

The funding from Research Nova Scotia and collaboration with MCC staff allowed researchers at NSCC-AGRG and the Dalhousie Statistics Department the ability to develop new tools to analysis return period of storm surge events. The observed water levels at various tide gauges in the region provide the best evidence of past sea levels to use in order to calculate the return periods of extreme events. We have shown how these return periods can be derived empirically from the observations using the annual block maxima technique and how they can be derived using extreme value models such as Gumbel. In addition to these estimates derived from the observed data we have also presented other sources of return periods that were based on 40-year and 65-year hindcasts of storm surge events to provide a time series that was used to calculate return periods. In the case of Bernier (2005) and Zhang and Sheng (2013) both hindcasts were driven by 6-hour time steps for the wind and pressure fields, thus potentially missing short-lived events like hurricanes which often cause coastal flooding in this region. Most recently Wang and Bernier (2025) used hourly data to generate the storm surges and calculate the 50-year and 100-year storm surge water level return periods.

We installed and replaced a damaged water level sensor that can be used by the MCC to measure water levels and start to build their own local time series of storm surge events.

We examined the water levels from the observations and hindcast derived models to determine the 20-year and 100-year coastal flood hazard for today and considering RSL in the future to 2050 and 2100 to build flood layers for the Northumberland and Fundy coasts of the MCC.

Acknowledgements

Graph figures were generated using the Matplotlib Python library.

References

Bernier, N. (2005). Annual and Seasonal Extreme Sea Levels in the Northwest Atlantic: Hindcasts over the Last 40 Years and Projections for the Next Century (Ph.D. Thesis). Halifax, Nova Scotia, Canada: Dalhousie University.

James, T.S., Robin, C., Henton, J.A., and Craymer, M., (2021). Relative sea-level projections for Canada based on the IPCC Fifth Assessment Report and the NAD83v70VG national crustal velocity model; Geological Survey of Canada, Open File 8764, 1 .zip file, https://doi.org/10.4095/327878

James. T, Brierley-Green. C. (in prep). “Intergovernmental Panel on Climate Change Sixth Assessment Report,” NRCan.

Richards, W. and Daigle, R. (2011). Scenarios and Guidance for Adaptation to Climate Change and Sea-Level Rise - NS and PEI Municipalities. Atlantic Climate Adaptation Solutions (ACAS), Nova Scotia Coastal Flood Risk Mapping Program.

Zhang. S, Sheng. J. (2013). “Estimation of Extreme Sea Levels Over the Eastern Continental Shelf of North America,” Geo Res: Oceans. 118, 6253-6273.

Wang, P., Bernier, N.B. (2025). Advancing global hindcast of extreme sea levels: Insights from a 65-year study. Weather and Climate Extremes, Volume 50, 2025, 100805, ISSN 2212-0947, https://doi.org/10.1016/j.wace.2025.100805. (https://www.sciencedirect.com/science/article/pii/S2212094725000635)

Webster, T, McGuigan, K., MacDonald, C. (2012). Lidar processing and Flood Risk Mapping for the Communities of the District of Lunenburg, Oxford-Port Howe, Town and District of Yarmouth, Chignecto Isthmus and Minas Basin. Atlantic Climate Adaptation Solutions (ACAS), Nova Scotia Coastal Flood Risk Mapping Program.

Appendix 1 Return Period Tables & Tidal Charts

Table 12 Storm surge water levels derived by AGRG from tide gauge observations in the region.

Station Code	Station Name	GEV Model Return Period (meters)		Empirical Return Period (meters)		Closest Empirical Points (years)	
		20 Year	100 Year	~20 Year	~100 Year	20 Year	100 Year
65	Saint John	1.34	1.65	1.36	2.04	21.40	107.00
365	Yarmouth	1.07	1.31	1.06	1.50	20.67	62.00
490	Halifax	1.17	1.40	1.13	1.67	19.40	97.00
491	Bedford Institute	1.32	1.36	1.27		14.00	
575	Port Hawkesbury	1.57	2.26	1.92		10.00	
612	North Sydney	0.99	1.13	1.04	1.04	18.33	55.00
1630	Pictou	2.19	2.22	2.11		19.00	
1700	Charlottetown	1.37	1.53	1.42	1.58	20.80	104.00
1805	Shediac Bay	1.95	2.27	1.99		21.50	

A comparison between Dalhousie University masters student, Fatma Sarhan, supervised by Dr. Orla Murphy with those derived by AGRG for the Shediac and Saint Joun tide gauges.

Table 13 Comparison of AGRG and Dalhousie (Fatma) derived storm surge return periods for Shediac.

Shediac Bay Residual Return Period Comparison			
Return Period (years)	Fatma (metres)	Gumbel (metres)	GEV (metres)
10	1.67	1.82	1.79
20	1.78	2.02	1.95
50	1.91	2.28	2.14
100	1.99	2.47	2.27

Table 14 Comparison of AGRG and Dalhousie (Fatma) derived storm surge return periods for Saint John.

Saint John Residual Return Period Comparison			
Return Period (years)	Fatma (metres)	Gumbel (metres)	GEV (metres)
10	1.04	1.20	1.20
20	1.22	1.33	1.34
50	1.49	1.51	1.52
100	1.74	1.64	1.65

Table 15 Compilation of various storm surge return periods in the region. See Figure 38 & Figure 39 for Zhang and Sheng (2013) and Wang and Bernier (2025) comparison.

Station Name	25 year Richards & Daigle	50 year Richards & Daigle	100 year Daigle	Observed Residual	Event	Wang and Bernier 50 year Gumbel	Wang and Bernier 100 year Gumbel	Zhang and Sheng 50 year unfiltered	Zhang and Sheng 100 year unfiltered	HHWLT CGVD 2013
Saint John	0.8	0.87	0.94	1.28	Goundhog Day 1977	1.03	1.105	0.78	0.79	
Yarmouth	0.75	0.81	0.87	1.29	Goundhog Day 1976	0.87	0.92	0.82	0.88	
Halifax	0.81	0.88	0.95	1.63	Juan 2003	0.98	1.05	0.83	1.01	
Pictou	1.27	1.38	1.49	1.38	30-Dec-93	1.6	1.72	1.39	1.49	
Charlottetown	1.3	1.42	1.55	1.37	21-Jan-00	1.4	1.5	1.23	1.33	
Shediac Bay	1.54	1.69	1.83	2.20	Fiona 9/22/2022	2.05	2.23	1.43	1.48	0.656
Upper Fundy	0.96	1.04	1.13	2	Saxby 1869	1.48	1.6	2.51	2.8	6.41
	Joggins	Joggins	Joggins							
	1.01 Burntcoat Head	1.1 Burntcoat Head	1.2 Burntcoat Head			0.94	1	2.43	2.55	7.38

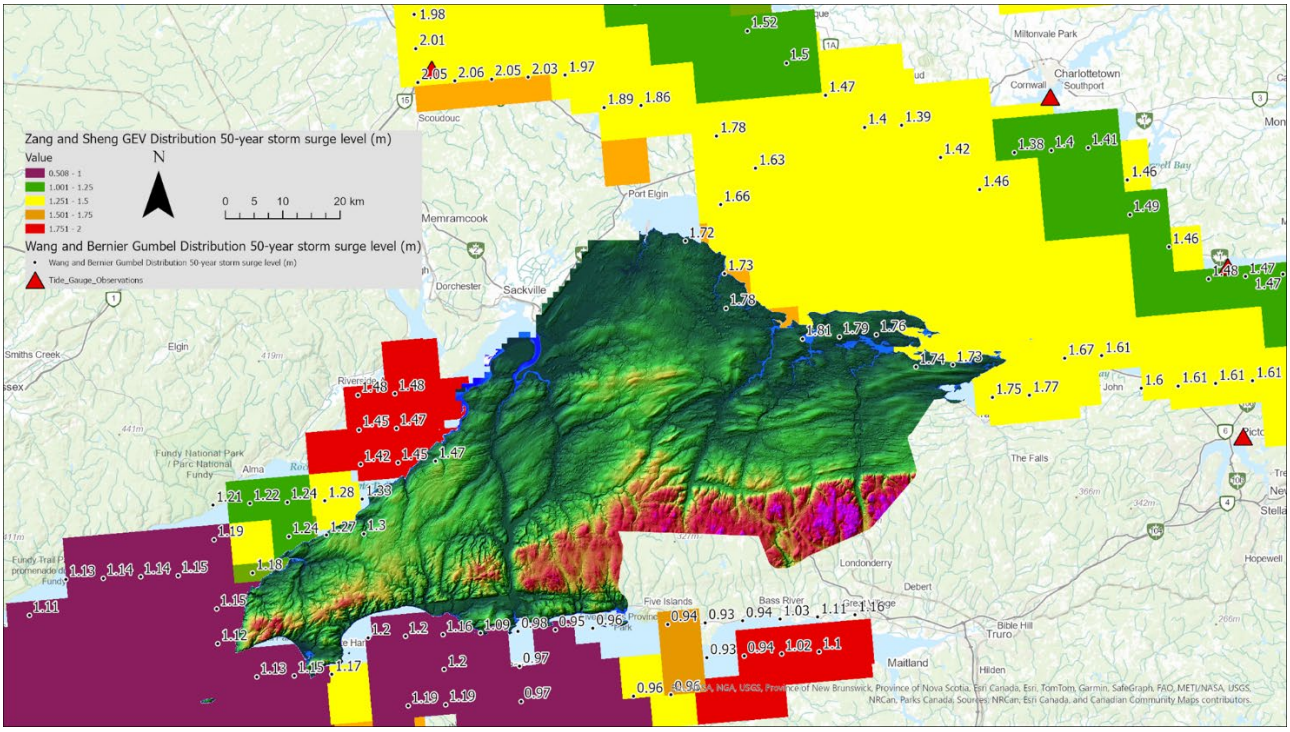

Figure 38 Comparison of Zhang and Sheng (2013) grid and the shoreline points from Wang and Bernier (2025) for the 50-year storm surge return period.

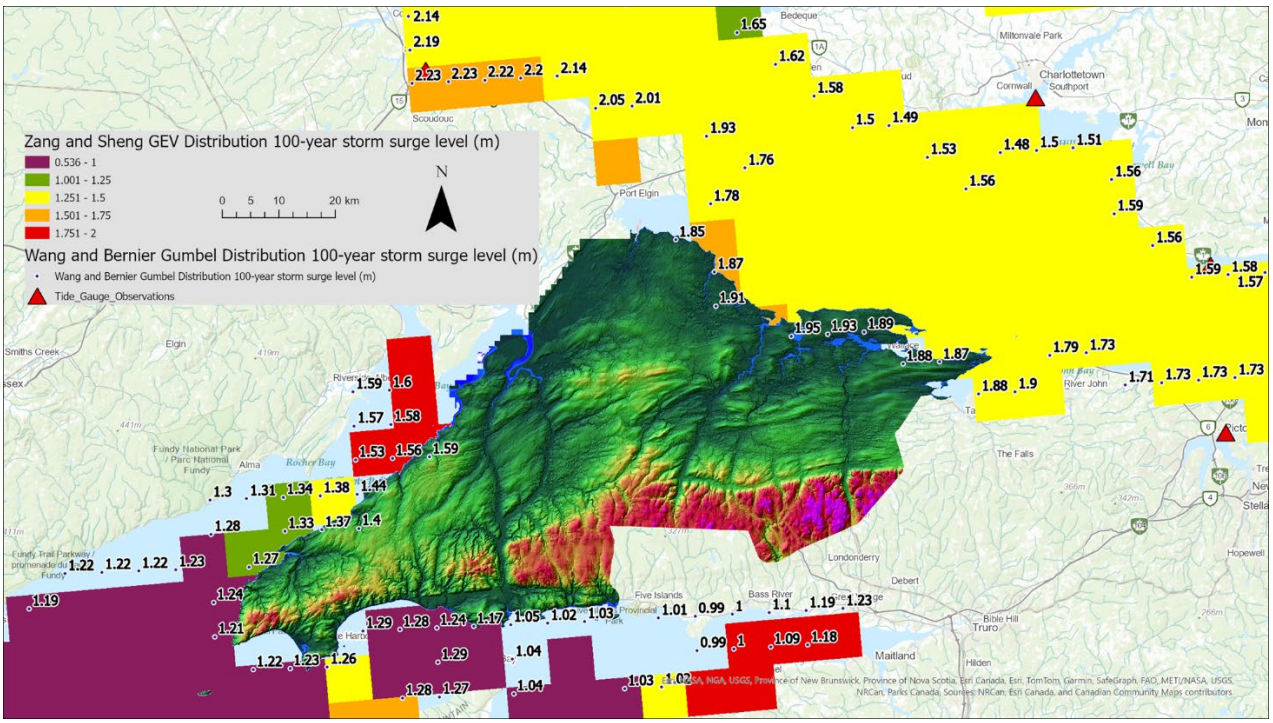

Figure 39 Comparison of Zhang and Sheng (2013) grid and the shoreline points from Wang and Bernier (2025) for the 100-year storm surge return period.

Table 16 Summary of coasts for the Municipality of the County of Cumberland.

	20 year Surge m	100 year Surge m	HHWLT M CGVD2013
Cumberland Northumberland	2	2.3	0.656
Cumberland Upper Bay of Fundy	2.08	2.8	6.41
Minas Basin	1.44	2.55	7.38

Table 17 Water levels to be considered in CGVD2013 for coastal hazard mapping. Final numbers used for mapping in beige cells.

	20-year TOTAL m CGVD2013	20-yr RSL 2050	20-yr RSL 2100	20-yr Antarctica sheet 2100	100-year TOTAL m CGVD2013	100-yr RSL 2050	100-yr RSL 2100	100-yr Antarctica sheet 2100
Cumberland Northumberland	2.656	3.096	3.896	4.546	2.956	3.396	4.196	4.846
Cumberland Upper Bay of Fundy	8.49	8.92	9.72	10.37	9.21	9.64	10.44	11.09
Minas Basin	8.82	9.25	10.05	10.7	9.93	10.36	11.16	11.81
FUNDY	15.55	15.98	16.78	17.43	18.225	19.085	20.685	21.985
	20-year	100-year	20-year 2050	100-year 2050	20-year 2100	100-year 2100	20-year 2100 + AA	100-year 2100 + AA
Northumberland	2.66	2.96	3.1	3.4	3.9	4.2	4.55	4.85
Fundy	15.55	18.23	15.98	19.09	16.78	20.29	17.43	21.99

Charlottetown Tide Gauge Analysis – Chart Datum is 1.21 m below CGVD2013

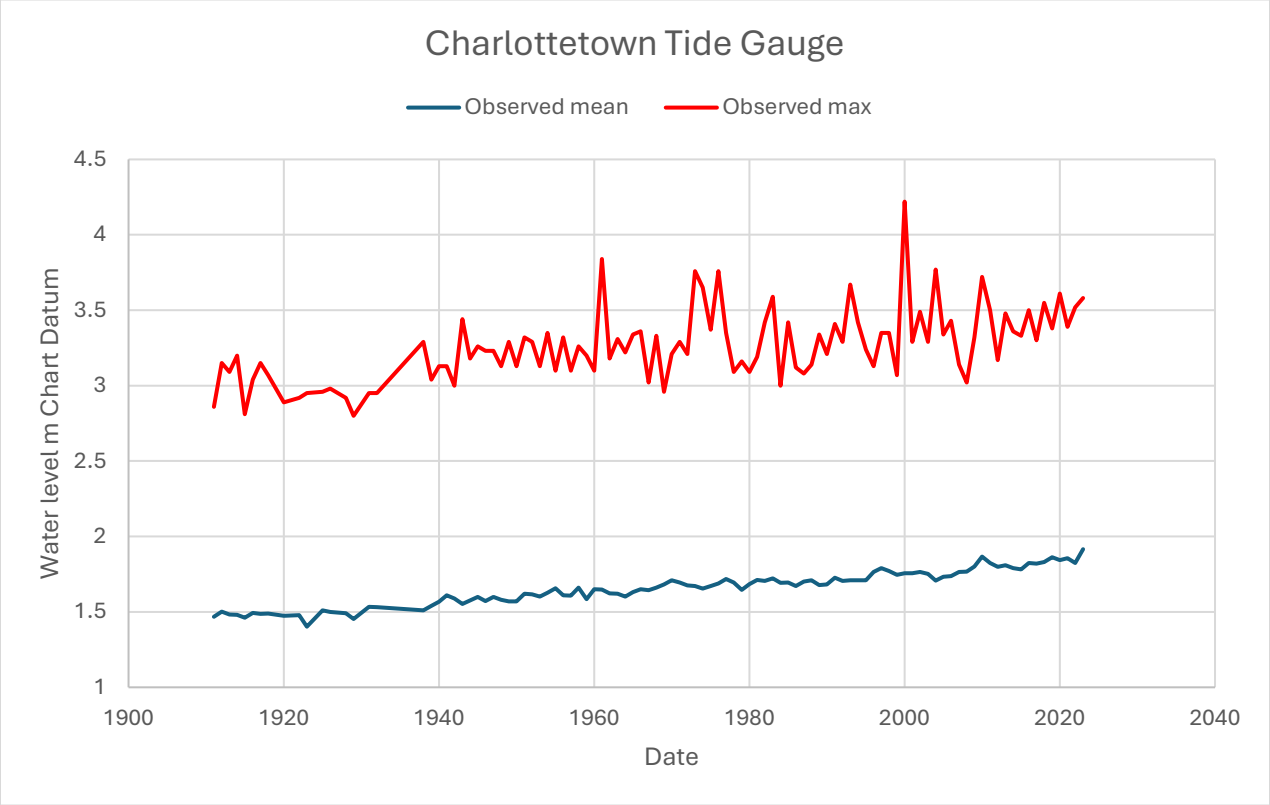

Figure 40 Charlotettown tide gauge annual maxima and mean water level m CD.

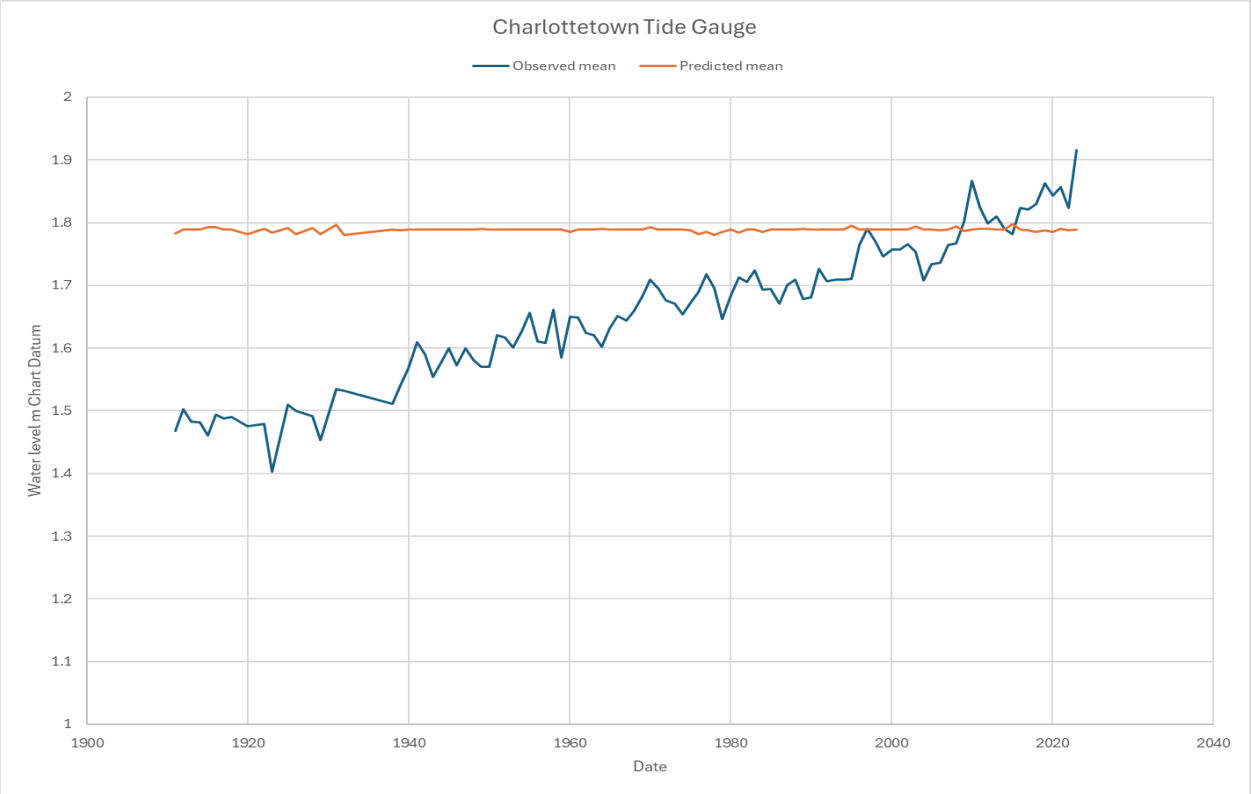

Figure 41 Charlottetown predicted annual mean and observed annual mean water level m CD. NOTE the slope of the observed data as a result of Relative Sea Level rise.

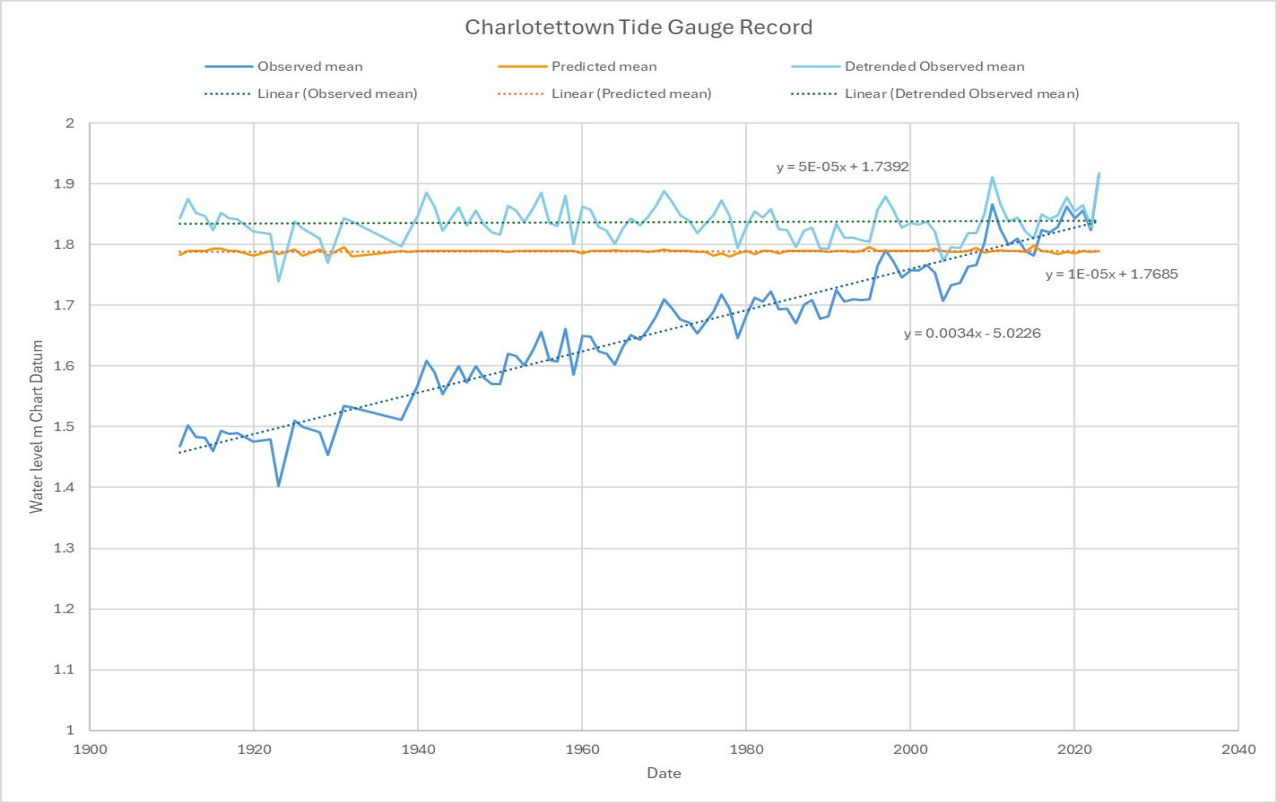

Figure 42 Charlotettown tide gauge with original and detrended observed annual mean water level and predcietd m CD.

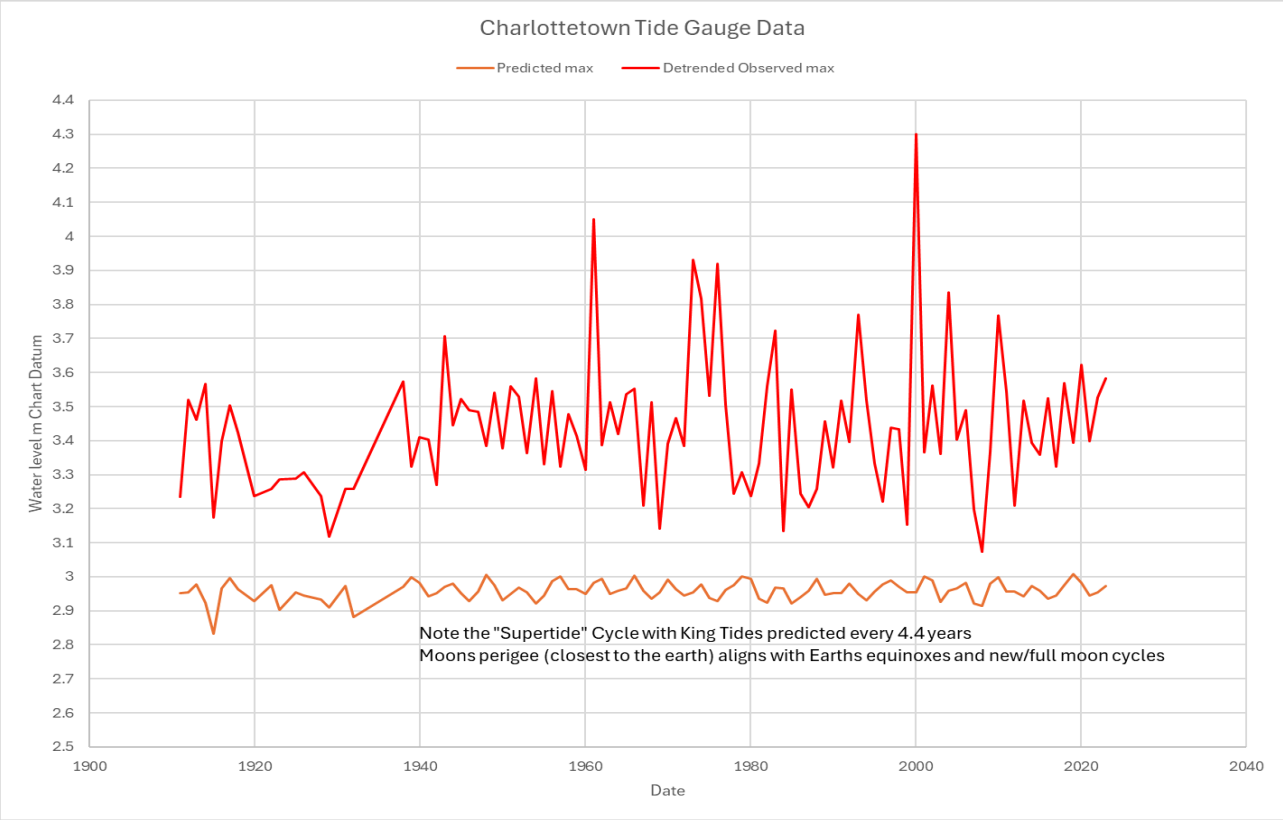

Figure 43 Charlottetown tide gauge annual detrended observed maxima and predicted annual maxima water level m CD.

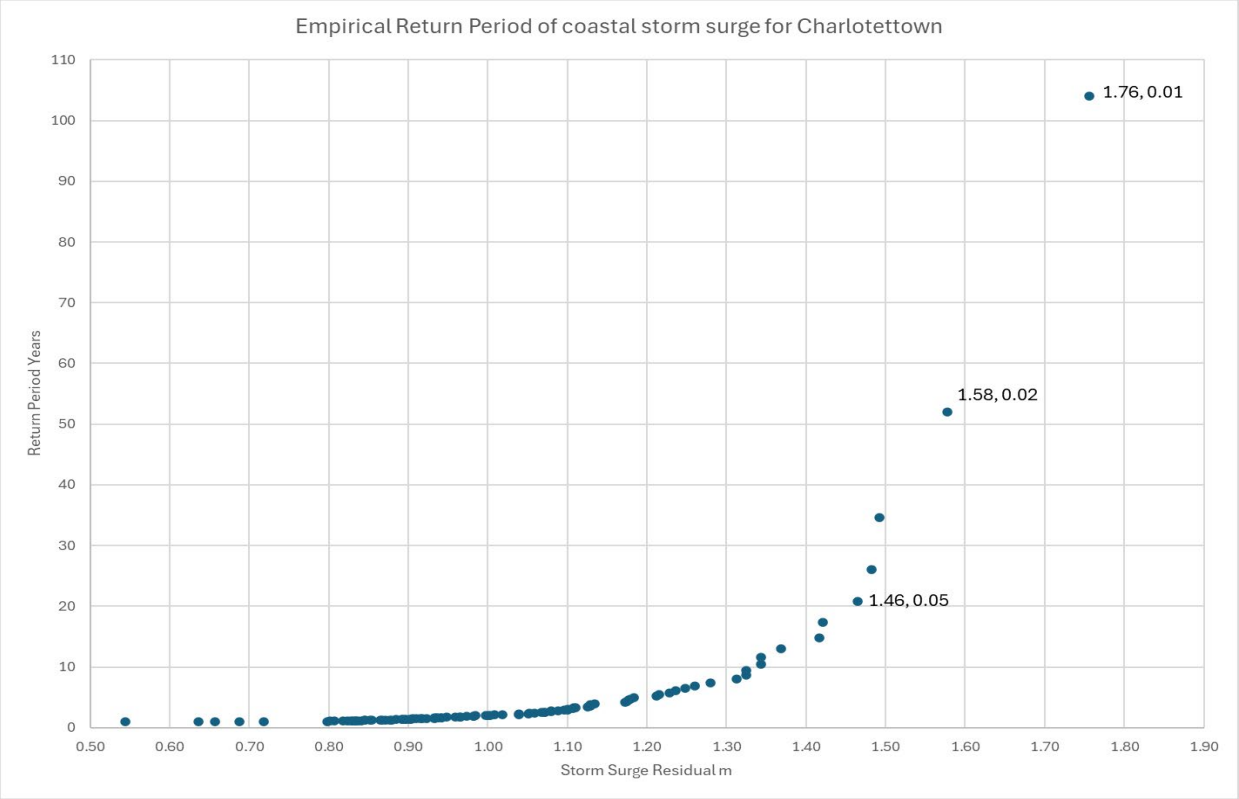

Figure 44 Charlotettown tide gauge emperically derived storm surge return periods. Labels are water level and annual exceedance probability.

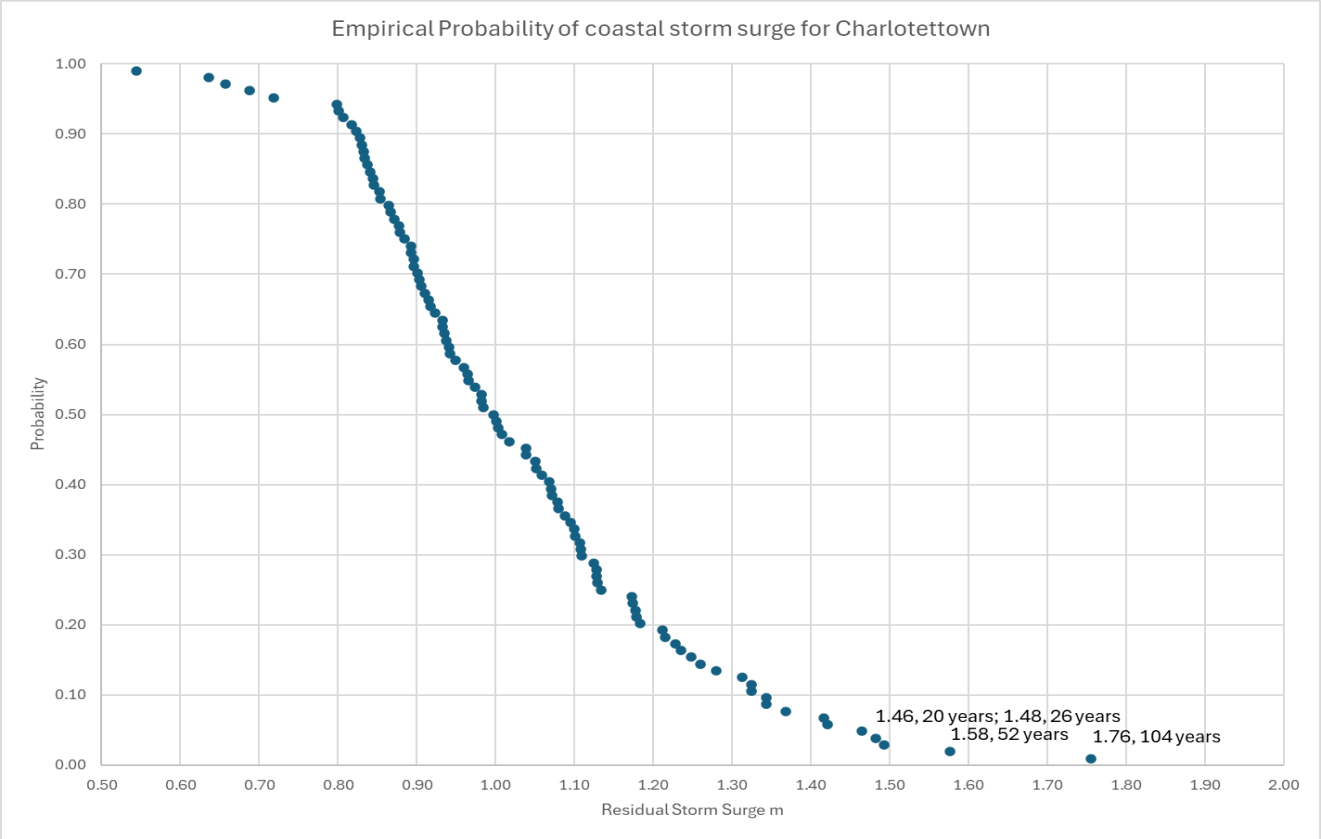

Figure 45 Charlotettown tide gauge emperically derived storm surge annual exceedance probability. Labels are water level and return period (years).

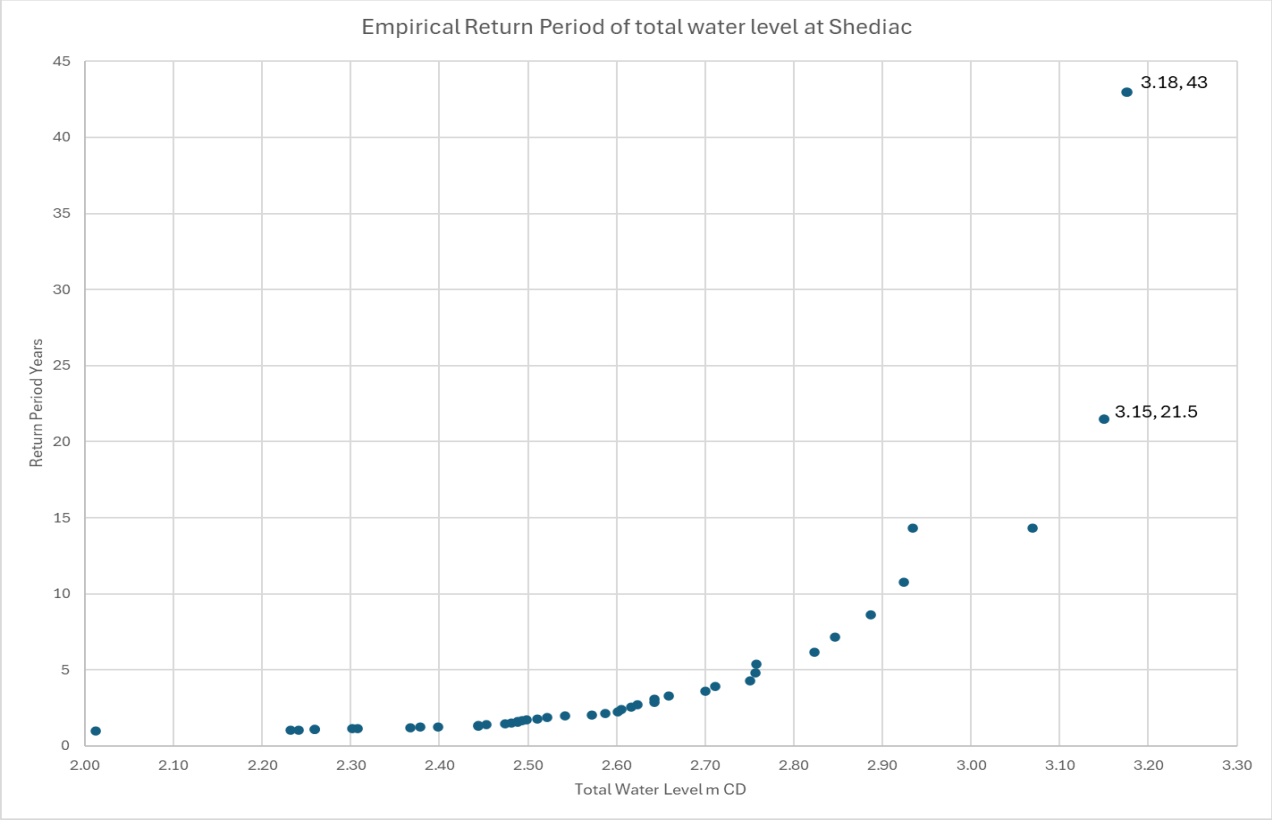

Figure 46 The Shediac-Point du Chene tide gauge emperically derived storm surge return periods. Labels are water level and retrun period (years).

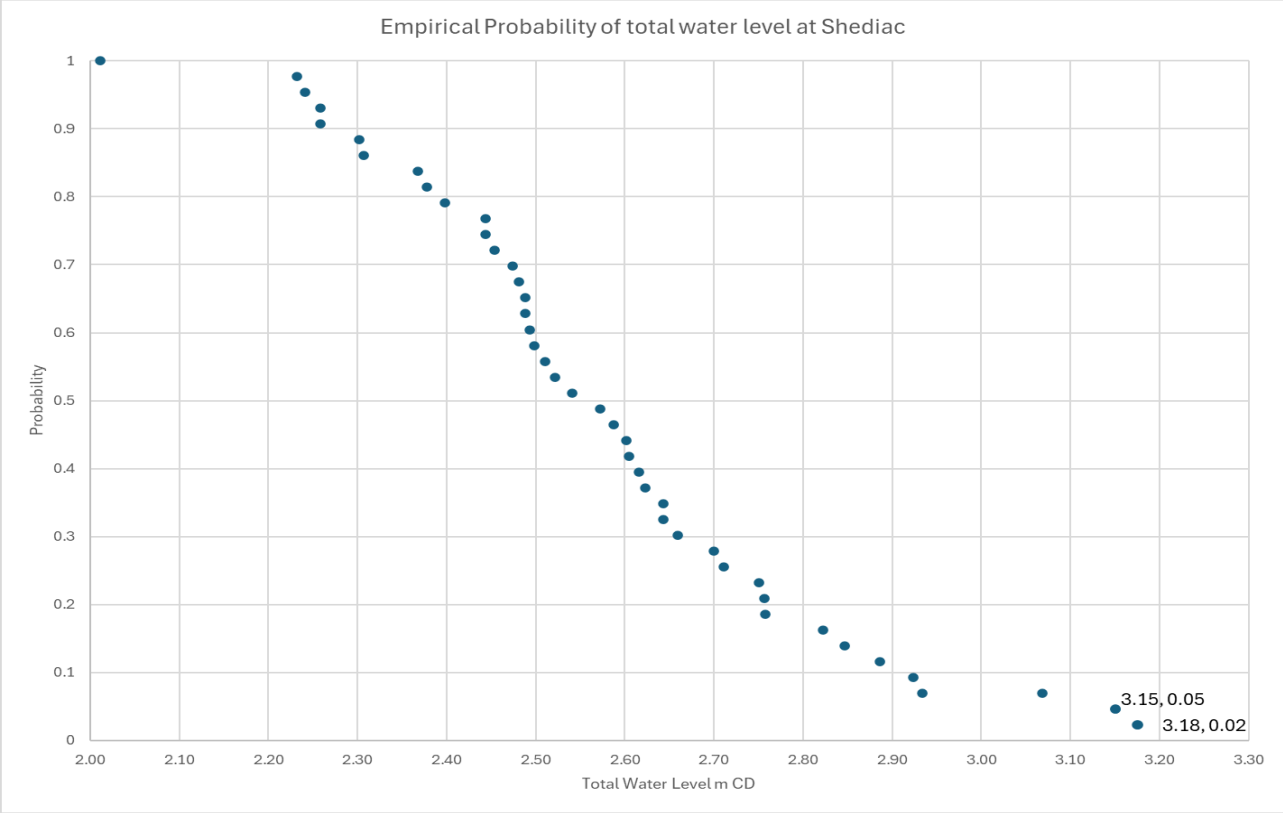

Figure 47 The Shediac-Point du Chene tide gauge emperically derived storm surge annual exceedance probability. Labels are water level and annual exceedance probability.

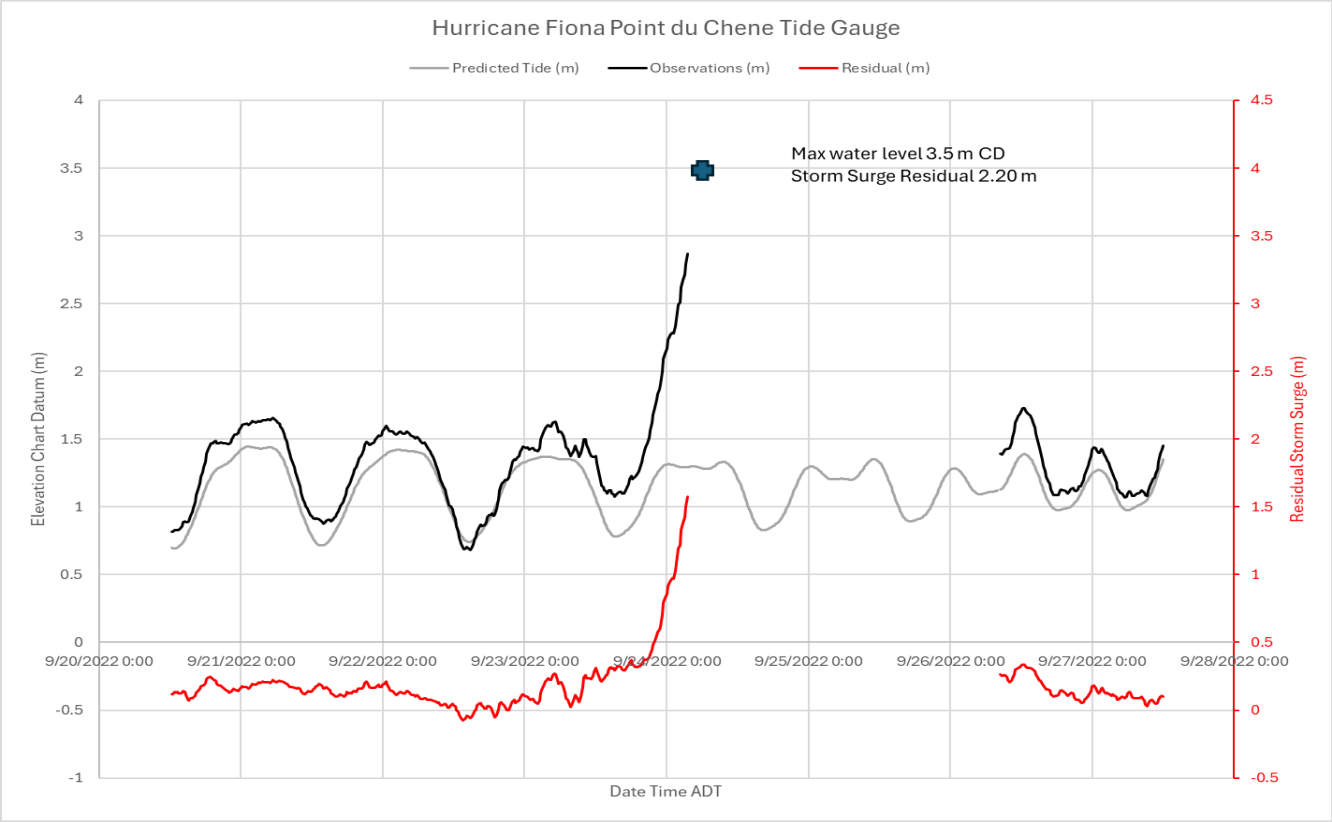

Figure 48 The Shediac-Point du Chene tide gauge during Hurricane Fiona. The CHS tide guage quite working before the maximun water level of 3.5 m was observed (m CD).

Appendix 2 – Dalhousie MSc summary

Statistical Report

March 2026

MSc Student: Fatma Sarhan
Co-supervisors: Dr. Orla Murphy and Dr. Jonathan Jalbert

Introduction

In recent years, Nova Scotia has experienced numerous flooding events triggered by thunderstorms, heavy rainfall, and other extreme weather conditions. Climate change projections indicate that such events are likely to increase in both frequency and intensity, posing a heightened risk of coastal flooding. These conditions have already had severe consequences, including evacuations, infrastructure damage, property loss, and even loss of life.

Modeling rare extreme events poses a significant challenge due to their infrequency, despite their profound societal and economic consequences. In extreme value analysis (EVA), coastal return levels are a quantification of risk and represent the water level that is expected to be exceeded once on average in a given time period, e.g., 50 years. Traditionally, these risks are estimated using univariate methods from EVA. Such methods analyze a coastal site individually to estimate return levels, and do not incorporate information from other nearby locations. As extreme events are rare, the available data for a single site is often sparse or incomplete, leading to high levels of uncertainty in the derived predictions. In addition, when extreme events are not modeled spatially, return level predictions are typically limited to locations with records.

To address these limitations and improve return level predictions, this study uses a model from EVA within a Bayesian Hierarchical Model (BHM) to model extreme coastal water levels spatially. While the univariate approach treats each location in isolation, the BHM allows for the sharing of information on extreme water levels spatially across different coastal locations while allowing for different record periods and lengths at each location. By borrowing strength from neighboring sites and incorporating atmospheric drivers (covariates) like wind speed and pressure, the BHM can provide an improved estimation of risk.

This report compares the univariate approach to a preliminary spatial BHM and outlines future proposed modifications to the BHM and results. An evaluation results from the univariate approach versus the spatial BHM approach demonstrates how the inclusion of regional data and covariates can reduce uncertainty. Intended return levels predictions at ungauged locations are also discussed.

Data Description and Exploration

This study incorporates data from eight key coastal locations in the Maritimes, primarily along the Nova Scotian coastline, as shown in Figure 1. The analysis utilizes raw hourly water level data extracted from the Government of Canada Data Archives as well as hourly pressure and wind speed predictions from the Canadian Surface Prediction Archive (CaSPAr), which were used as covariates within the BHM. Although water levels at several locations were recorded prior to 1980, this analysis focused on the period from 1980 to 2024 to match the CaSPAr covariate data. Furthermore, the water level records showed an upward trend due to rising sea levels. For modeling purposes, the linear trend was removed from the water levels prior to analysis. Different trends could be considered for future predictions.

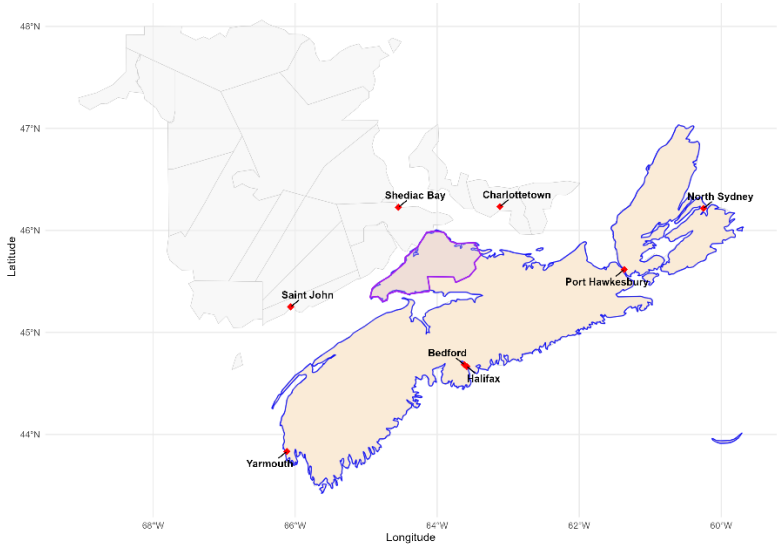

Figure 49: Map of the locations with water level records.

A common approach in EVA is to model annual maxima. It is important to note that years with more than 15% missing hourly data were excluded from the analysis to avoid biased estimation. This ensures that the annual maximum water levels identified for a given year are a proper representation of the strongest storm event, rather than an artifact of missing data. The resulting number of annual maxima per location ranged from 8 to 44 maxima. The variation in record length is a primary driver for choosing a BHM. This spatial approach allows us to use the long-term trends from data-rich sites to stabilize and improve the predictions for data-sparse locations.

To improve predicted return levels at locations with and without water level records, the covariates were included in the BHM. This work considered four key covariates which would improve prediction of extreme water levels: wind speeds at 10m and 20m levels as well as sea and surface level pressures. Different time windows between the covariates and extreme water levels were also considered resulting in the selection of the daily maximum wind speed at 20m above sea level and the daily minimum pressure both

recorded on the day before the annual peak. This exploratory investigation also implied that pressure is the more important predictor.

Figure 2 shows how the covariates correlate with annual water level maxima using Bedford as an example. The full set of correlation plots for the remaining locations, along with the full correlation summary table, can be found in the Appendix.

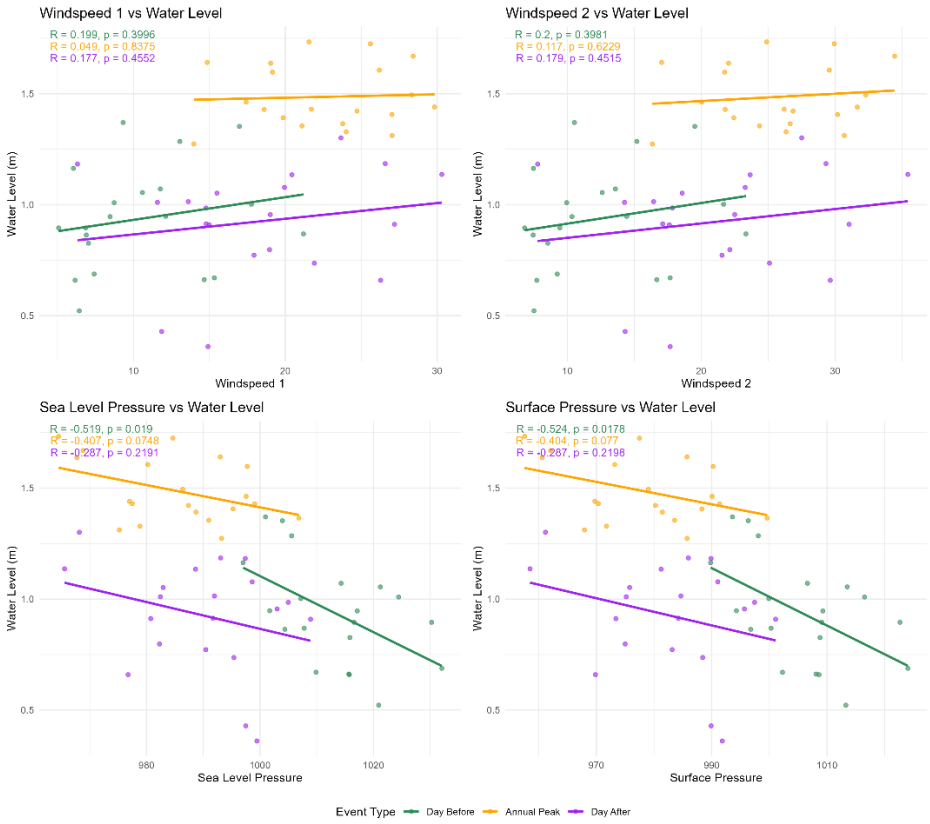

Figure 2: Correlation analysis between annual maximum water levels (m) at Bedford and the covariates: Wind Speeds 1 and 2 (10m and 20m levels, respectively) and Atmospheric Pressure (Sea Level and Surface). Each panel displays the relationship across a three-day window centered on the annual water level peak, categorized as the Day Before (Green), the Annual Peak (Orange), and the Day After (Purple).

Model Comparison and Results

This section compares results between the BHM and univariate (denoted by MLE) approaches. Table 1 summarizes their 50-year return level estimates, the width of the corresponding 95 % intervals, and the difference between the interval widths between the two approaches. In the univariate EVA approach, the generalized extreme value (GEV) distribution is fit to each individual location's set of annual maxima separately. Return level estimates are computed for each location's estimated model along with their associated 95% confidence intervals. In the BHM approach, two of the GEV parameters (location and scale) are allowed to vary across space, while the final parameter (shape) is fixed across all locations. To inform the location and scale parameters, the model incorporates the atmospheric covariates: surface pressure and wind speed (20m). Specifically, for each

location, the average of the annual minimum pressures and maximum wind speeds recorded on the days before the annual water level peaks are incorporated.

Table 18: 50-year return level estimates and intervals from the univariate and BHM analyses with associated 95% intervals for all study locations.

Location	BHM Return Level	MLE Return Level	BHM 95% credible interval width	MLE 95% confidence interval width	Diff (BMH - MLE)
Bedford	1.799	1.8314	0.3148	0.6510	-0.3362
Charlottetown	2.090	2.1815	0.1718	0.5815	-0.4097
Halifax	1.672	1.6850	0.2159	0.3297	-0.1138
North Sydney	1.296	1.3271	0.1395	0.1768	-0.0373
Port Hawkesbury	1.5402	1.4722	0.3039	0.0730	0.23102
Saint John	4.6133	4.6691	0.1556	0.3189	-0.1632
Shediac Bay	1.9251	2.0838	0.4094	1.0517	-0.6423
Yarmouth	2.912	3.0048	0.1381	0.4743	-0.3361

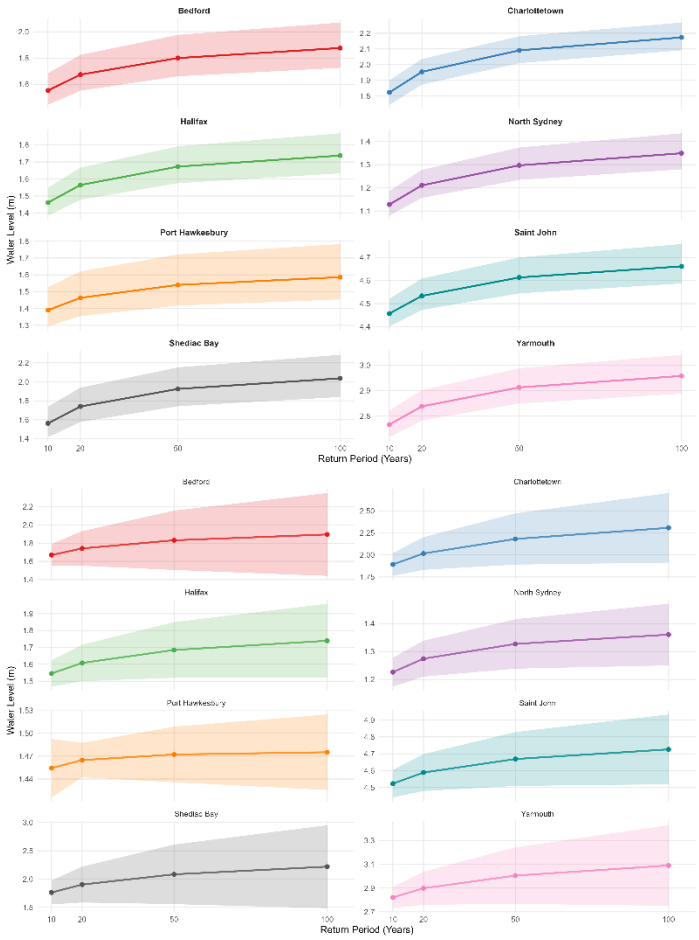

Figure 3: Visual comparison plots of return level estimates and associated uncertainty for 10-, 20-, 50-, and 100-year return periods between the spatial BHM and univariate models for all study locations.

From the above Figure 3, it is evident that for the majority of the study locations, such as Shediac Bay and Charlottetown, there is a reduction in the uncertainty intervals from the BHM compared to the univariate MLE approach. This tightening of the intervals demonstrates the power of the BHM in stabilizing predictions by borrowing strength from regional data.

Next Steps

The current model establishes a baseline by utilizing the average of the annual maximum and minimum covariates to summarize the environmental drivers at each location. However, it can be further improved by allowing the covariates to change across time. Transitioning to this upgraded model would be more sensible given the results reached from the exploratory analysis. This would allow the model to leverage significantly more information per location, capturing how year-to-year fluctuations in weather intensity directly influence the magnitude of extreme water levels.

Ultimately, the current results provide a strong framework for generating return level estimates across the entire coast of Nova Scotia. As in, the finalized relationships between GEV parameters and covariates can be used to predict return levels at ungauged locations, such as the Municipality of the County of Cumberland, as covariate information is available all along the Nova Scotian coastline.

Year vs Processed Annual Water Level Maxima for all locations.

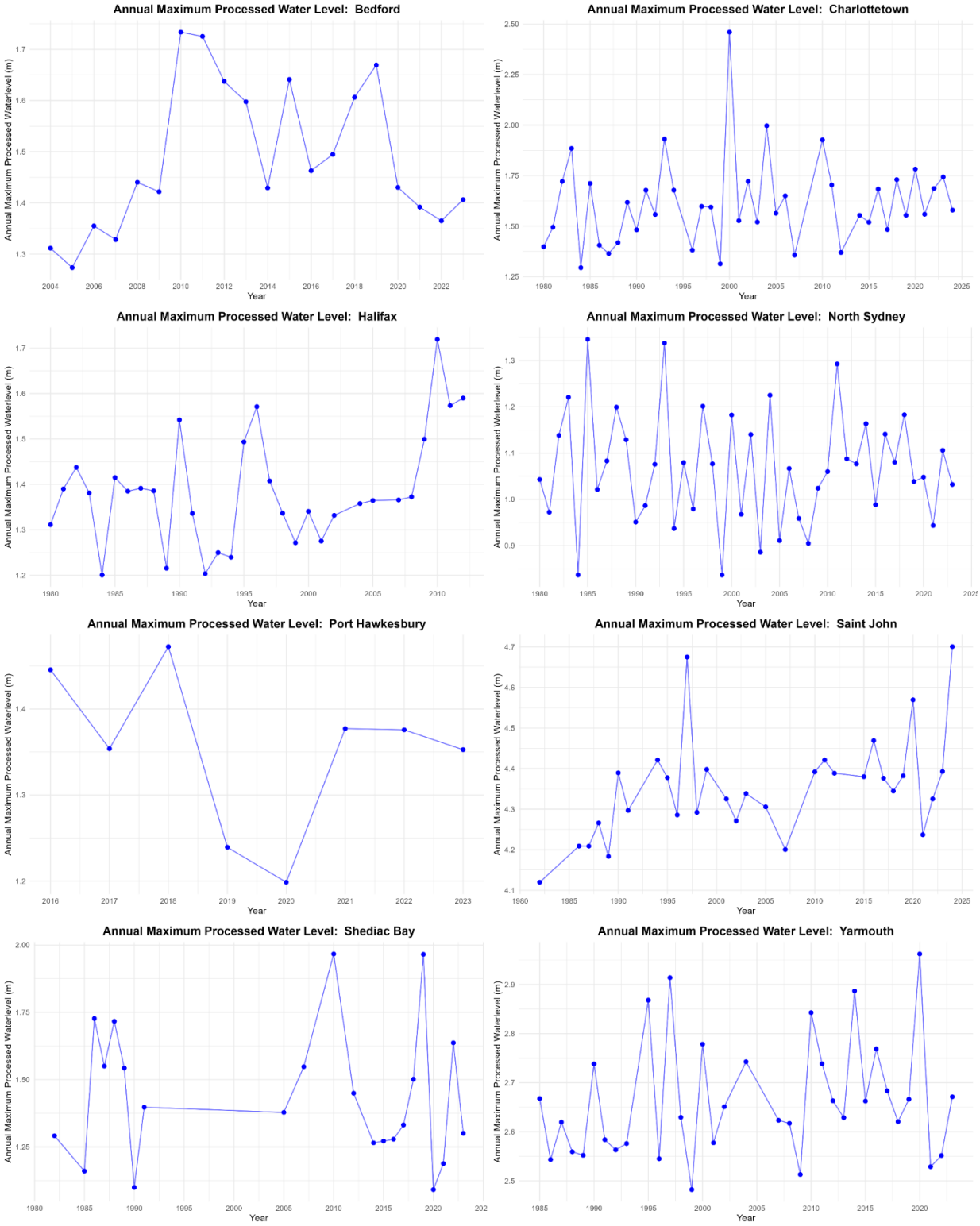

Summary Table for the number of annual maxima.

Location	Number of Annual Max Water Levels
Bedford	20
Charlottetown	41
Halifax	31
North Sydney	44
Port Hawkesbury	8
Saint John	30
Shediac Bay	22
Yarmouth	35

Correlation Exploration Plots: The four previously identified covariates vs the annual water level maximas at the exact grid cell of each of the locations.

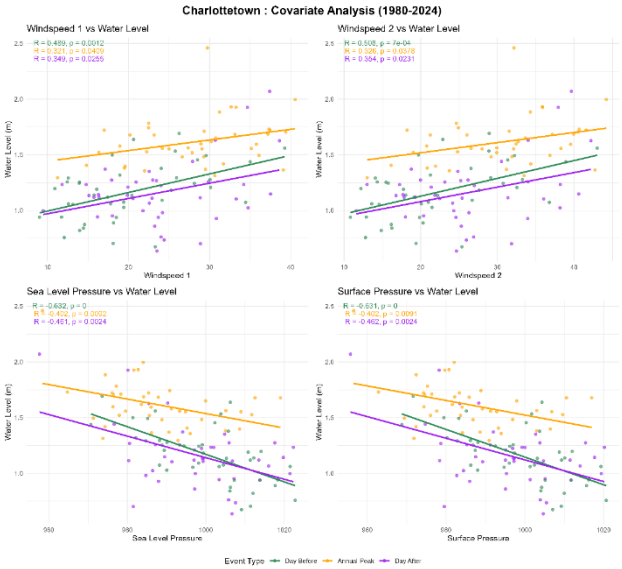

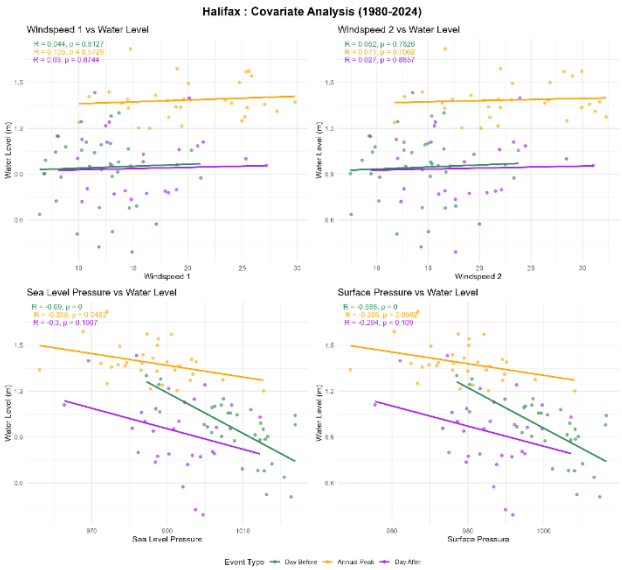

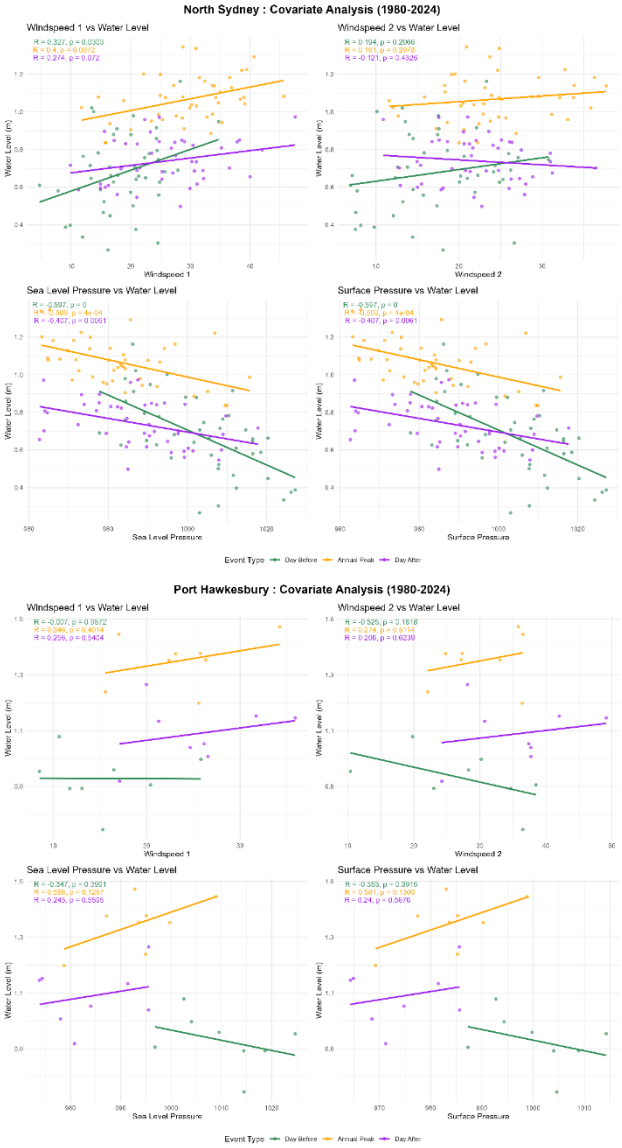
North Sydney : Covariate Analysis (1980-2024)
Windspeed 1 vs Water Level
R = 0.327, p = 0.0303
R = 0.4, p = 0.0072
R = 0.274, p = 0.072
Windspeed 2 vs Water Level
R = 0.194, p = 0.2066
R = 0.161, p = 0.2978
R = -0.121, p = 0.4526
Sea Level Pressure vs Water Level
R = -0.597, p = 0
R = -0.369, p = 4e-04
R = -0.407, p = 0.0061
Surface Pressure vs Water Level
R = -0.597, p = 0
R = -0.369, p = 4e-04
R = -0.407, p = 0.0061
Water Level (m)
Windspeed 1
Windspeed 2
Sea Level Pressure
Surface Pressure
Event Type
Day Before
Annual Peak
Day After
Port Hawkesbury : Covariate Analysis (1980-2024)
Windspeed 1 vs Water Level
R = -0.007, p = 0.9872
R = 0.346, p = 0.4014
R = 0.256, p = 0.5404
Windspeed 2 vs Water Level
R = -0.525, p = 0.1618
R = 0.274, p = 0.5134
R = 0.206, p = 0.6239
Sea Level Pressure vs Water Level
R = -0.347, p = 0.3951
R = -0.086, p = 0.7857
R = 0.249, p = 0.5935
Surface Pressure vs Water Level
R = -0.353, p = 0.3916
R = 0.081, p = 0.8369
R = 0.24, p = 0.5976
Water Level (m)
Windspeed 1
Windspeed 2
Sea Level Pressure
Surface Pressure
Event Type
Day Before
Annual Peak
Day After

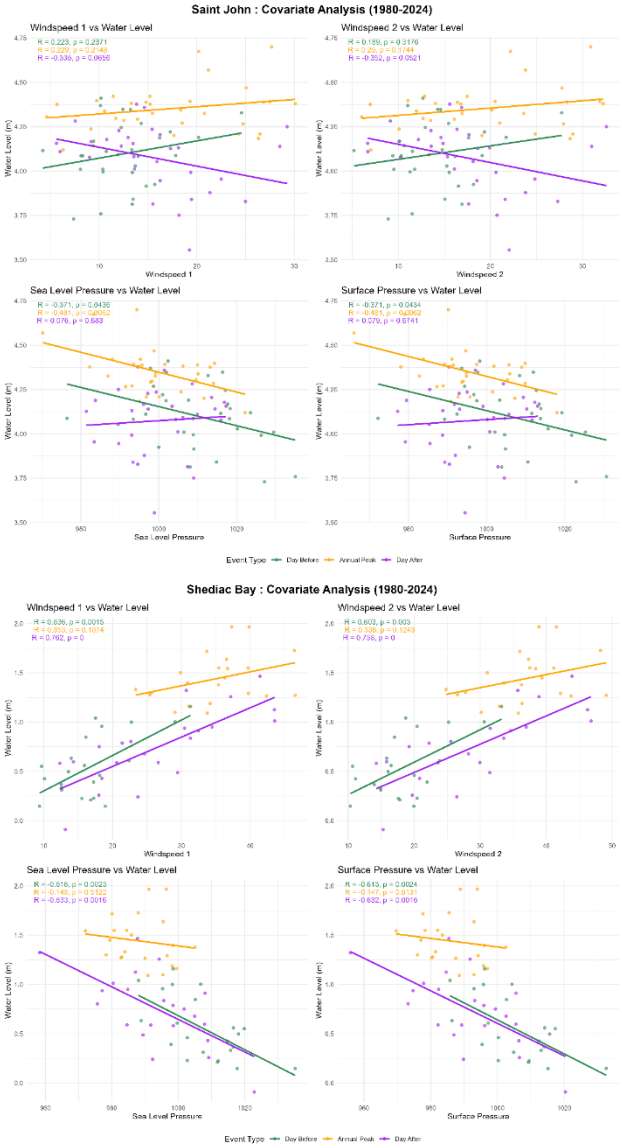
Saint John : Covariate Analysis (1980-2024)
Windspeed 1 vs Water Level
Windspeed 2 vs Water Level
Sea Level Pressure vs Water Level
Surface Pressure vs Water Level
Water Level (m)
Windspeed 1
Windspeed 2
Sea Level Pressure
Surface Pressure
Event Type
Day Before
Annual Peak
Day After
Shediac Bay : Covariate Analysis (1980-2024)
Windspeed 1 vs Water Level
Windspeed 2 vs Water Level
Sea Level Pressure vs Water Level
Surface Pressure vs Water Level
Water Level (m)
Windspeed 1
Windspeed 2
Sea Level Pressure
Surface Pressure
Event Type
Day Before
Annual Peak
Day After

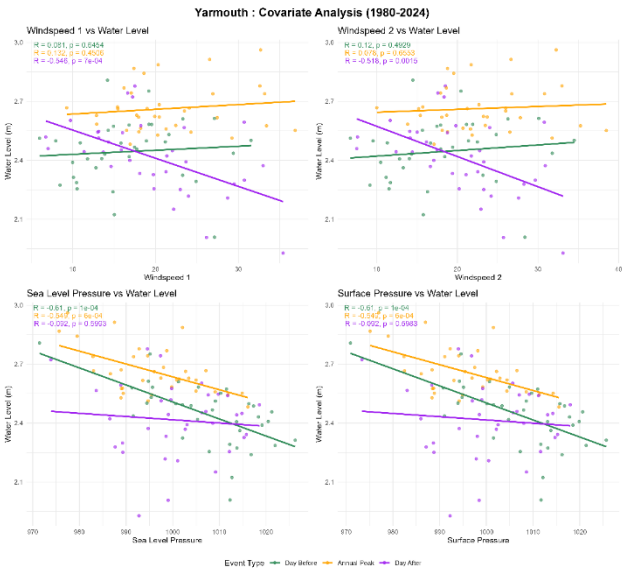

Full Correlation Summary Table.

Location	Event_Type	Covariate	Pearson_R	P_Value
Bedford	Day Before	Max_Windspeed1	0.199279201	0.399611
Bedford	Annual Peak	Max_Windspeed1	0.048990686	0.837488
Bedford	Day After	Max_Windspeed1	0.177042325	0.455241
Bedford	Day Before	Max_Windspeed2	0.199888946	0.39814
Bedford	Annual Peak	Max_Windspeed2	0.117135541	0.62285
Bedford	Day After	Max_Windspeed2	0.17850718	0.451459
Bedford	Day Before	Min_Pressure	-0.519084548	0.01901
Bedford	Annual Peak	Min_Pressure	-0.407122015	0.074819
Bedford	Day After	Min_Pressure	-0.287489019	0.21905
Bedford	Day Before	Min_SurfPressure	-0.523834989	0.017758
Bedford	Annual Peak	Min_SurfPressure	-0.404318984	0.077038
Bedford	Day After	Min_SurfPressure	-0.287038692	0.219805
Charlottetown	Day Before	Max_Windspeed1	0.489005576	0.001177
Charlottetown	Annual Peak	Max_Windspeed1	0.320730169	0.040901
Charlottetown	Day After	Max_Windspeed1	0.348527932	0.025536
Charlottetown	Day Before	Max_Windspeed2	0.508052672	0.000696
Charlottetown	Annual Peak	Max_Windspeed2	0.32552417	0.037815
Charlottetown	Day After	Max_Windspeed2	0.354141614	0.023107
Charlottetown	Day Before	Min_Pressure	-0.631768615	9.43E-06
Charlottetown	Annual Peak	Min_Pressure	-0.401924349	0.009191
Charlottetown	Day After	Min_Pressure	-0.461301972	0.0024
Charlottetown	Day Before	Min_SurfPressure	-0.631300178	9.62E-06
Charlottetown	Annual Peak	Min_SurfPressure	-0.402240719	0.009131
Charlottetown	Day After	Min_SurfPressure	-0.461581419	0.002384
Halifax	Day Before	Max_Windspeed1	0.044347109	0.812747

Halifax	Annual Peak	Max_Windspeed1	0.105313489	0.572865
Halifax	Day After	Max_Windspeed1	0.029591019	0.874441
Halifax	Day Before	Max_Windspeed2	0.051642414	0.782624
Halifax	Annual Peak	Max_Windspeed2	0.070522768	0.706182
Halifax	Day After	Max_Windspeed2	0.026910689	0.885737
Halifax	Day Before	Min_Pressure	-0.689771731	1.77E-05
Halifax	Annual Peak	Min_Pressure	-0.357556711	0.048289
Halifax	Day After	Min_Pressure	-0.30030082	0.100708
Halifax	Day Before	Min_SurfPressure	-0.685588142	2.08E-05
Halifax	Annual Peak	Min_SurfPressure	-0.354746502	0.050207
Halifax	Day After	Min_SurfPressure	-0.293559504	0.108969
North Sydney	Day Before	Max_Windspeed1	0.326915245	0.030312
North Sydney	Annual Peak	Max_Windspeed1	0.399851025	0.007163
North Sydney	Day After	Max_Windspeed1	0.273867757	0.072034
North Sydney	Day Before	Max_Windspeed2	0.194164696	0.206616
North Sydney	Annual Peak	Max_Windspeed2	0.160557484	0.297815
North Sydney	Day After	Max_Windspeed2	-0.121359817	0.432605
North Sydney	Day Before	Min_Pressure	-0.597232017	1.87E-05
North Sydney	Annual Peak	Min_Pressure	-0.509308118	0.000414
North Sydney	Day After	Min_Pressure	-0.40732377	0.006066
North Sydney	Day Before	Min_SurfPressure	-0.597249946	1.87E-05
North Sydney	Annual Peak	Min_SurfPressure	-0.50933166	0.000414
North Sydney	Day After	Min_SurfPressure	-0.407313787	0.006067
Port Hawkesbury	Day Before	Max_Windspeed1	-0.006850737	0.987155
Port Hawkesbury	Annual Peak	Max_Windspeed1	0.345857222	0.401375
Port Hawkesbury	Day After	Max_Windspeed1	0.256092609	0.540408
Port Hawkesbury	Day Before	Max_Windspeed2	-0.524752117	0.181791
Port Hawkesbury	Annual Peak	Max_Windspeed2	0.27397431	0.511426
Port Hawkesbury	Day After	Max_Windspeed2	0.20635407	0.62393
Port Hawkesbury	Day Before	Min_Pressure	-0.347435669	0.399084
Port Hawkesbury	Annual Peak	Min_Pressure	0.586273247	0.126654
Port Hawkesbury	Day After	Min_Pressure	0.244515888	0.559479
Port Hawkesbury	Day Before	Min_SurfPressure	-0.352615148	0.391606
Port Hawkesbury	Annual Peak	Min_SurfPressure	0.581115647	0.130857
Port Hawkesbury	Day After	Min_SurfPressure	0.239642309	0.567577
Saint John	Day Before	Max_Windspeed1	0.222596512	0.237083
Saint John	Annual Peak	Max_Windspeed1	0.229238012	0.214793
Saint John	Day After	Max_Windspeed1	-0.334834842	0.065589
Saint John	Day Before	Max_Windspeed2	0.188842129	0.317596
Saint John	Annual Peak	Max_Windspeed2	0.250298648	0.174442
Saint John	Day After	Max_Windspeed2	-0.352069937	0.05209
Saint John	Day Before	Min_Pressure	-0.370955476	0.043578
Saint John	Annual Peak	Min_Pressure	-0.480764281	0.006187

Saint John	Day After	Min_Pressure	0.076365717	0.683046
Saint John	Day Before	Min_SurfPressure	-0.37122201	0.043416
Saint John	Annual Peak	Min_SurfPressure	-0.480868975	0.006174
Saint John	Day After	Min_SurfPressure	0.078637802	0.674123
Shediac Bay	Day Before	Max_Windspeed1	0.635592662	0.001478
Shediac Bay	Annual Peak	Max_Windspeed1	0.352680211	0.107424
Shediac Bay	Day After	Max_Windspeed1	0.761579907	3.83E-05
Shediac Bay	Day Before	Max_Windspeed2	0.603044841	0.00297
Shediac Bay	Annual Peak	Max_Windspeed2	0.33767853	0.124305
Shediac Bay	Day After	Max_Windspeed2	0.758066019	4.36E-05
Shediac Bay	Day Before	Min_Pressure	-0.616385369	0.002252
Shediac Bay	Annual Peak	Min_Pressure	-0.147590418	0.512174
Shediac Bay	Day After	Min_Pressure	-0.633383242	0.001554
Shediac Bay	Day Before	Min_SurfPressure	-0.612997263	0.002419
Shediac Bay	Annual Peak	Min_SurfPressure	-0.147258358	0.513134
Shediac Bay	Day After	Min_SurfPressure	-0.632092699	0.0016
Yarmouth	Day Before	Max_Windspeed1	0.080575405	0.645424
Yarmouth	Annual Peak	Max_Windspeed1	0.131743664	0.450611
Yarmouth	Day After	Max_Windspeed1	-0.546454785	0.000683
Yarmouth	Day Before	Max_Windspeed2	0.119830369	0.49293
Yarmouth	Annual Peak	Max_Windspeed2	0.078180362	0.655302
Yarmouth	Day After	Max_Windspeed2	-0.517541617	0.001453
Yarmouth	Day Before	Min_Pressure	-0.61017471	9.95E-05
Yarmouth	Annual Peak	Min_Pressure	-0.548984546	0.000638
Yarmouth	Day After	Min_Pressure	-0.091970545	0.599263
Yarmouth	Day Before	Min_SurfPressure	-0.61028737	9.91E-05
Yarmouth	Annual Peak	Min_SurfPressure	-0.549314442	0.000632
Yarmouth	Day After	Min_SurfPressure	-0.092215636	0.598286